

CHAPTER IV

RESULTS

Solvents used for extracting polyphenols in TaSH

Tamarind seed husks (TaSH) were easily separated TaSH by drying. The obtained dried TaSH were used for extraction. Three different methods of extraction were applied in this study. For the preliminary method, TaSH was extracted using ethanol/water (7:3, v/v) at room temperature according to the study by Pumthong (1999). In the second method, TaSH was extracted using acetone/ water (7:3, v/v) at room temperature, followed by Sephadex LH20 column chromatography. The extract prepared by the second method was also used for silica gel column chromatography. The second extraction method was aimed to prepare the fractions of small molecular weight polyphenolic compounds from TaSH. The third method, TaSH was extracted with ethanol/water (3:2, v/v) at 60°C for 24 hours one time (one pot extraction) and three times (three time repeated extraction). Both extracts were further purified using Sephadex LH20. The third method was designed to investigate the polymer of proanthocyanidins contained in TaSH. All extracts described were dried under the reduced pressure at 50-60°C and by freeze-drying, yielding dark brown and non-hygroscopic powder.

The percent yield of ethanol extract (TE) in the first method and acetone extract (TA) in the second methods was 28% and 35%, respectively. The percent yield of one pot extraction and the three times repeated extractions were $43.5 \pm 2.0\%$ and $47 \pm 1.8\%$, respectively.

TA completely dissolved in ethanol but did not completely dissolve in water or phosphate buffer saline (PBS) at 1mg/ml. Phenolic content in TA dissolved in PBS was about half of the phenolic content dissolved in ethanol (Table 4).

Table 4 Phenolic content in TA by Folin Ciocalteu method

Samples	Phenolic content as gallic acid equivalent* (mg of gallic acid/mg of sample)
Catechin	1.51 ± 0.03
TA (in the case of using ethanol for solvent)	0.62 ± 0.02
TA (in the case of using PBS for solvent)	0.35 ± 0.01

* mean ± SD

Qualitative and quantitative analysis of condensed tannins in TA

1. Qualitative analysis of polyphenols, flavonoids and condensed tannins in TA

Table 5 shows chemical components of TA comparing with commercial grape seed extract (GSE). Phenolic compounds and flavonoids are abundantly present in both TA and GSE using Folin-Ciocalteu and Cyanidin reactions, respectively (Table 5). Tannin identification methods such as ferric chloride, gelatin and bromine water also showed positive results in both TA and GSE. A red colour of product after hydrolysis with acid and acid butanol indicated the presence of condensed tannins. Carbohydrate in both TA and GSE were slightly found according to Molisch’s test. Pew test of TA and GSE showed no flavanonol or flavonol-3-glycoside.

Table 5 Qualitative chemical characterizations of tamarind seed husk extract using aqueous acetone (TA) and grape seed extract (GSE)

Method	Test for	Occurrences of TA	Occurrences of GSE
Folin Ciocalteu	Phenols	+++	+++
Cyanidin reaction	Flavonoids	+++	+++
Molisch's test	Carbohydrate	+	+
Acid hydrolysis	Condensed tannin	+++	+++
Acid butanol test	Condensed tannin	+++	+++
Ferric chloride test	Tannin	+++	+++
Gelatin	Tannin	+++	+++
Bromine water	Tannin	+++	+++
Vanillin method	Flavan (Flavanol)	++	++
Pew test	Flavanonol	-	-

Remark: (-) = Absent, (+) = slightly present, (++) = fairly present, (+++) = abundantly present

2. Quantitative determination and relative degree of polymerization of condensed tannins in TA

The extract was treated with acid butanol to cleave interflavan bond. The TA yielded significantly higher levels of condensed tannin than the GSE standard (Table 6). For example at a concentration of 50µg/ml TA showed yield of 4 -fold greater than GSE. Vanillin reacts with meta-substituted A-ring of flavanols (flavan-3-ol) in a terminal unit of condensed tannins to form chromophore. This method was widely used for analysis of proanthocyanidins (Yamakoshi, et al., 2002). The flavanols level in TA was also significantly higher than GSE (Table 6).

The relative degree of polymerization (DP) can be estimated by comparing the absorbance of the modified vanillin assay (due to terminal flavan-3-ol units) with the absorbance of the acid butanol method (due to total oligomeric flavan-3-ol residues) (Butler, 1982; Hagerman, 1998). Table 6 summarized these data and indicated that the average degree of polymerization of the condensed tannins in TA (6.03) was essentially the same as the level of polymerization in GSE (6.19).

Table 6 The relative degree of polymerization of TA comparing with GSE

Samples	E 1% Acid	E 1% Vanillin	Relative Degree of
	Butanol	Assay	Polymerization
TA	509.68	84.49	6.03
GSE	142.98	23.10	6.19

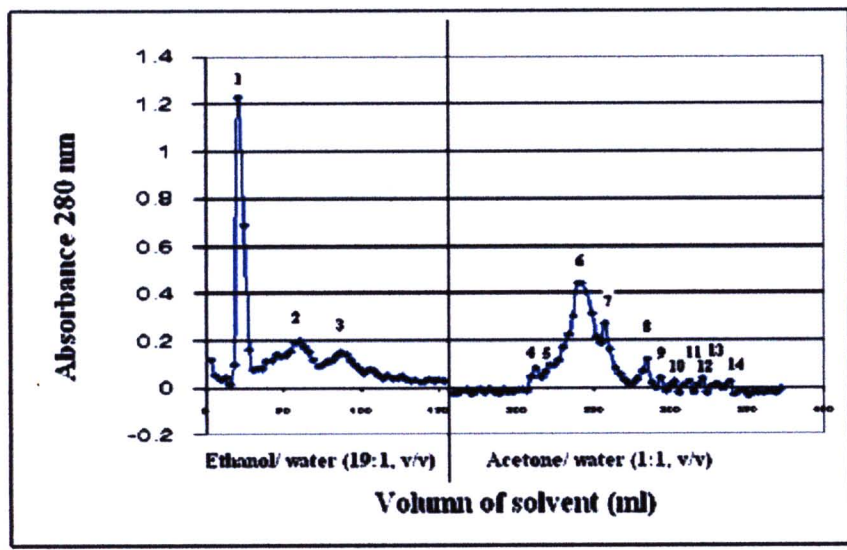
Remark: $E = A / CI$ (E = extinction coefficient, A = absorbance, I = cell path length in cm, usually 1 and C = concentration of samples in g/ liter)

3. Chromatograms of TA purification using Sephadex LH20 column chromatography

TA which dissolved in ethanol/water (19:1, v/v) was applied on top of Sephadex LH20 column. The first preliminary column was eluted with the mobile phase of ethanol/water (1:1) and acetone/water (1:1, v/v). The fractions were collected and determined by measuring optical density of phenolic compounds at 280 nm. The chromatogram of TA fractions eluted from column was shown in Figure 17a. There were at least three phenolic compounds (fractions number 1-3) in ethanolic fraction of TA (eTAS). The overlapping peak of acetone fraction (number 1-7) indicated the mixture of phenolic compounds. Each fraction of eTAS and aTAS was analyzed by thin-layer chromatography (TLC) developed with toluene: acetone: formic acid (6: 6:

1, v/v) according to Lea (1978) (Figure 17b). Separated antioxidative components were visualized by DPPH spraying. In Figure 28b, some mobile antioxidative molecules (fraction 1 of eTAS) and other compounds with no antioxidant activity (fraction 2-3 of eTAS) were eluted by ethanol/water (19:1, v/v). From the spots of TLC, there were at least three antioxidative compounds in aTAS. In the case of proanthocyanidins, the spot which stays in the origin in this TLC system should be the polymeric proanthocyanidins, while the moving spots should be monomeric or oligomeric proanthocyanidins (OPCs) according to the report of Lea (1978).

(a)



(b)

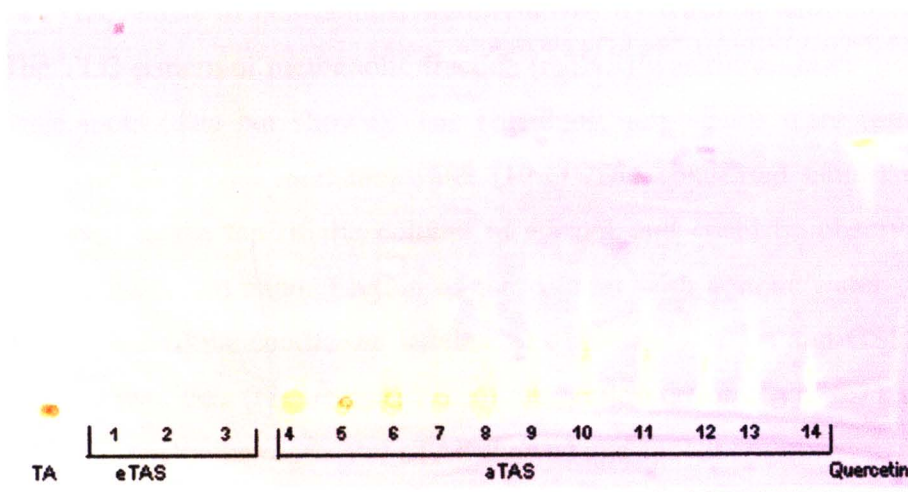


Figure 17 The fractions (number 1-14) of TaSH purification from Sephadex LH20 column chromatography elute with ethanol/water (19:1, v/v) and acetone/water (1:1, v/v). (a) Chromatogram of TA purification determined the absorbance at 280nm, (b) TLC analysis compared between TA, eTAS (number 1-3) and aTAS using toluene: acetone: formic acid (6: 6: 1, v/v/v) as mobile phase (number 4-14).

For the second purification, TA was chromatographed on Sephadex LH20 with ethanol/water (19:1, v/v), methanol/water (19:1, v/v) and acetone/water (1:1, v/v). The detector of the system was connected to the column and continuously detected their multi absorbance. However, the absorbance at 226 and 279 could not be detected in acetone fractions because of interference by acetone absorbance. The UV/VIS spectrums of each fraction are shown in Appendix D.

The fractions of TA which were purified by Sephadex LH 20 were detected the absorbance at 226, 279, 450 and 506 nm (Figure 18). The UV spectrums of general flavanoids have two peaks at 240-285 nm (ring A) and 300-550 nm (ring B). Chromatogram of TA and GSE purification from Sephadex LH20 column chromatography showing the absorbance value are revealed in Appendix C. The purification chromatograms of TA and GSE are in the same pattern (Figure 18). As illustrated by the chromatogram in Figure 28-30, when TA was applied to column of Sephadex LH20, some of non-tannins were removed by washing with ethanol/water (19:1). The TLC pattern of methanolic fraction (mTAS) was shown both moving and non-moving spots (data not shown). The remaining non-tannins were removed by exhaustively washing with methanol/water (19:1). The condensed tannin remained tightly adsorbed to the top of the column in ethanol and could be observed as an immobile, orange-brown band. Elution of the column with acetone/water (1:1, v/v) subsequently released the condensed tannins. The similarity of TA and GSE on TLC chromatograms was clear (Figure 19). A spot at retention factor (R_f) of 0.71 should be catechin. The TLC chromatogram of aTAS showed one spot at origin.

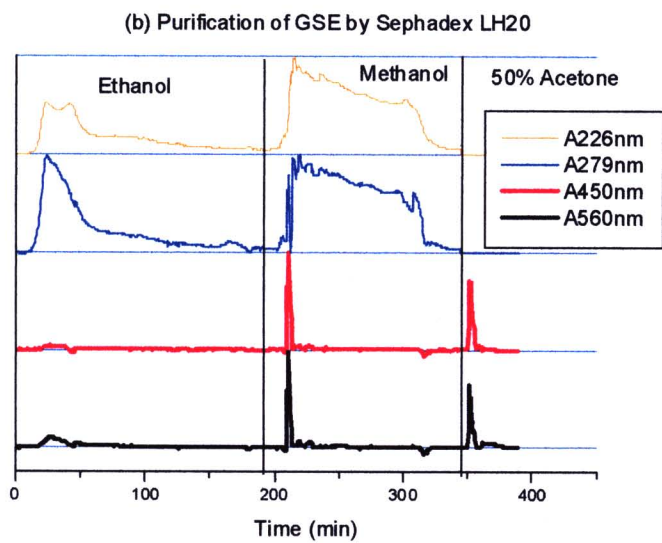
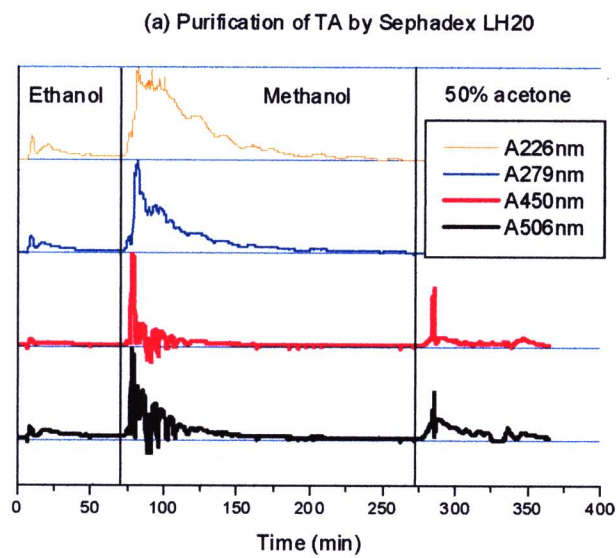


Figure 18 Chromatogram of TA (a) and GSE (b) purification using Sephadex LH 20 column chromatography eluted with ethanol/water (19:1, v/v), methanol/water (19:1, v/v) and acetone/water (1:1, v/v), respectively. The optical density of fractions was continuously determined at 226,279,450,506 nm. The graphs are normalization chromatogram of TA plot between absorbance and time (min).

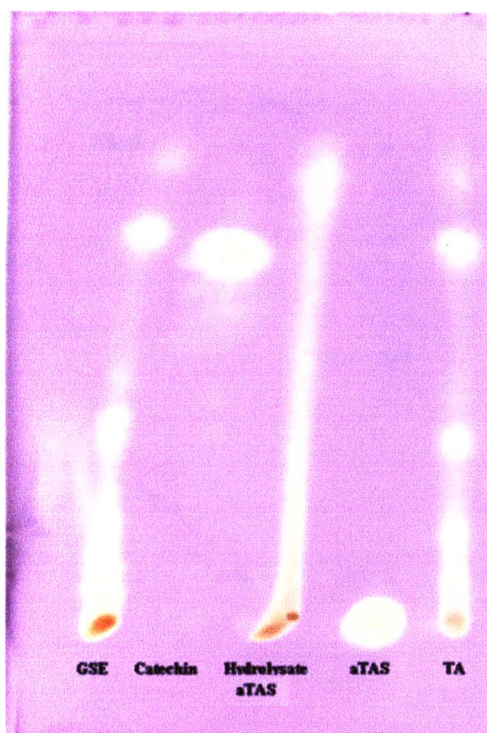


Figure 19 TLC chromatogram of GSE, catechin, hydrolysate aTAS, aTAS and TA using toluene/acetone/formic acid (6: 6:1, v/v/v) as mobile phase

Chemicals characterization of flavonoids and condensed tannins in TA

1. IR spectrums of flavonoids in TA, aTAS, and hydrolysed aTAS

The IR spectra of TA (Figure 20) had identical absorption pattern comparing with that of GSE (Figure 21) and both of them contained the all necessary groups of flavonoids. The IR spectrum shape of GSE and TA were difference from that of gallic acid (Figure 22) which was non-flavonoids phenolic compounds.

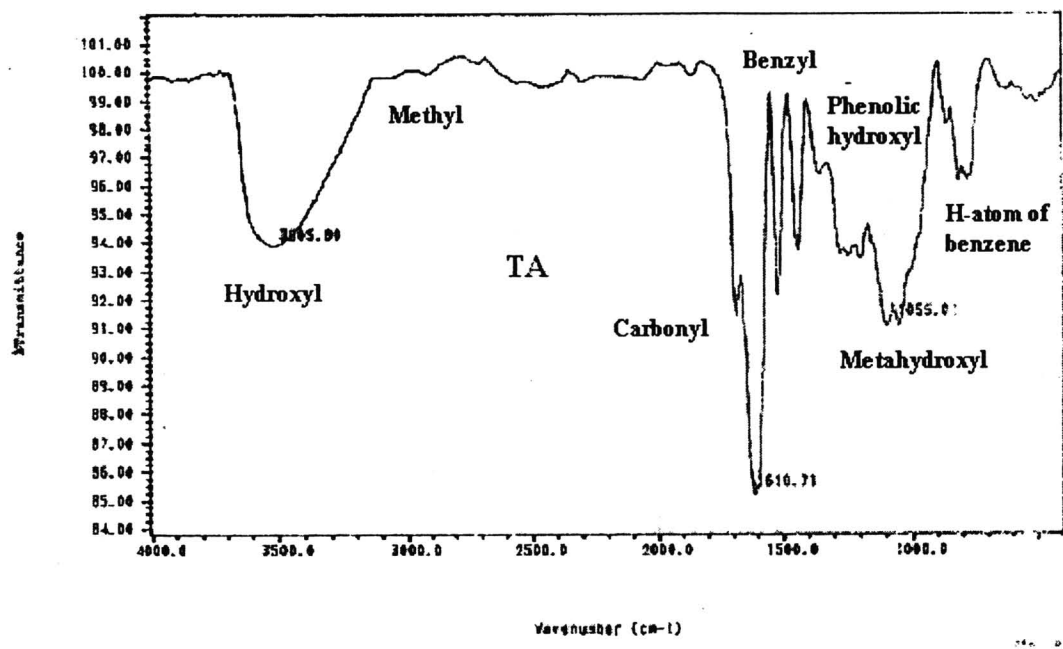


Figure 20 Infrared spectrums of flavonoids in TA using KBr disc

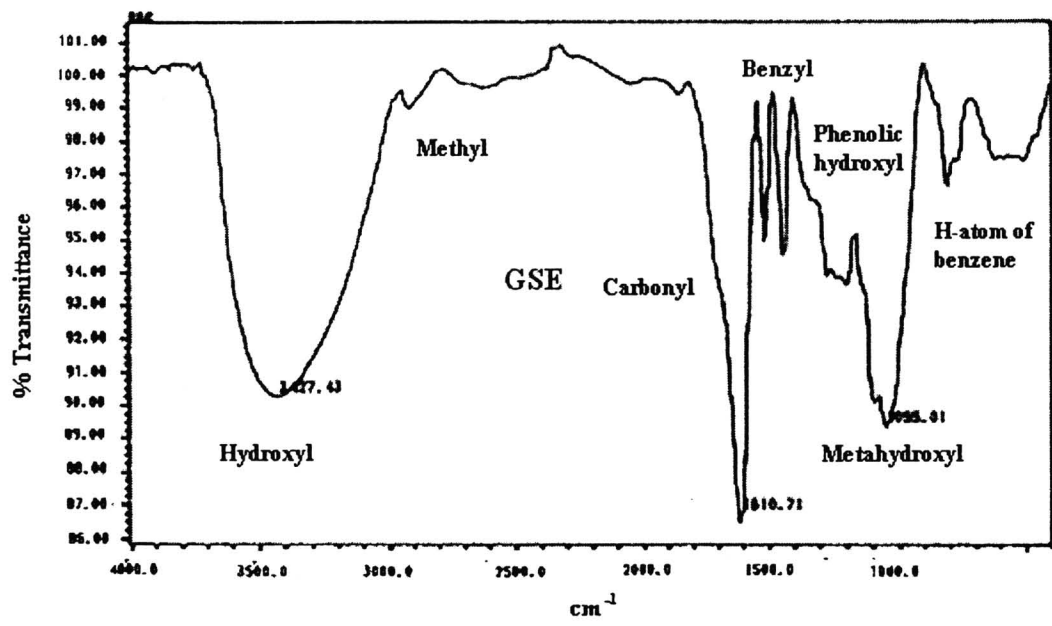


Figure 21 Infrared spectrums of oligomeric proanthocyanidins in GSE using KBr disc

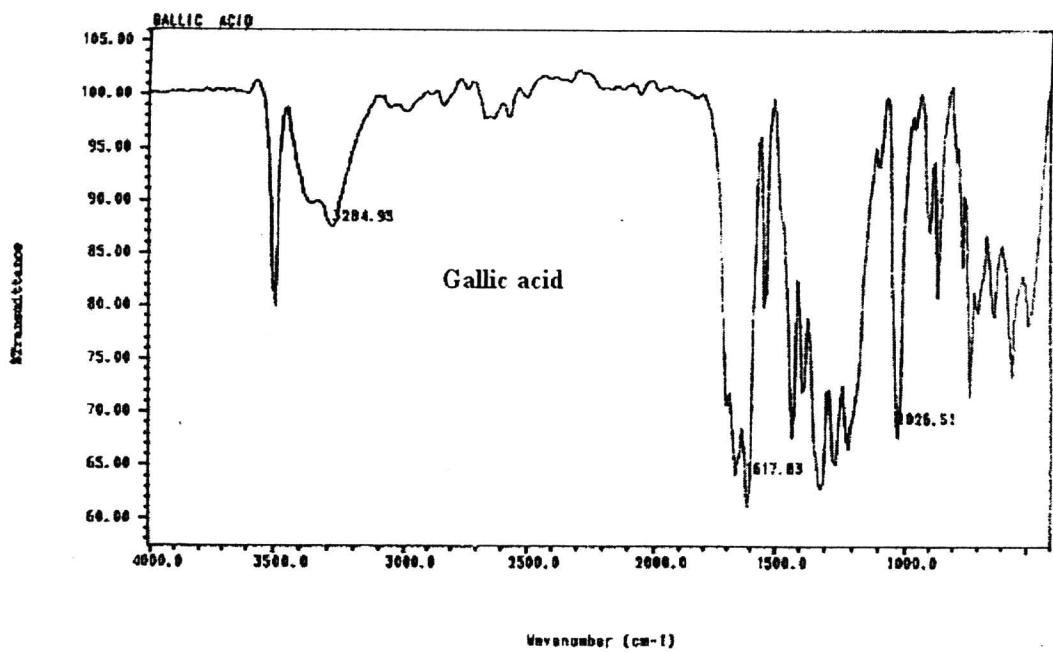


Figure 22 Infrared spectrums of gallic acid (non-flavonoid phenolic compound) using KBr disc

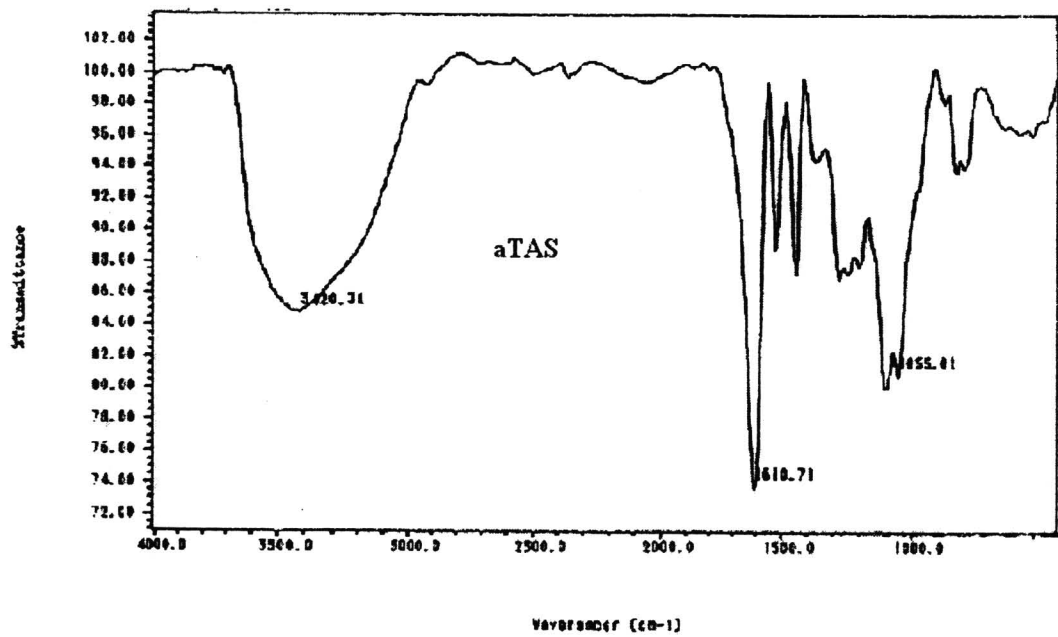


Figure 23 Infrared spectrums of flavonoids in aTAS using KBr disc

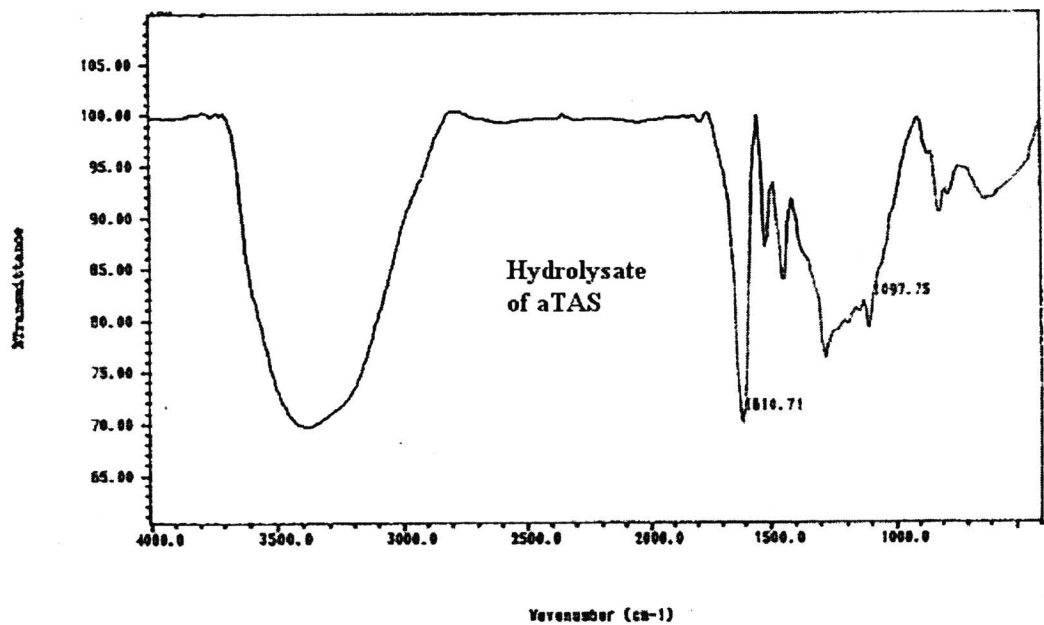


Figure 24 Infrared spectrums of flavonoids in hydrolysate of aTAS using KBr disc

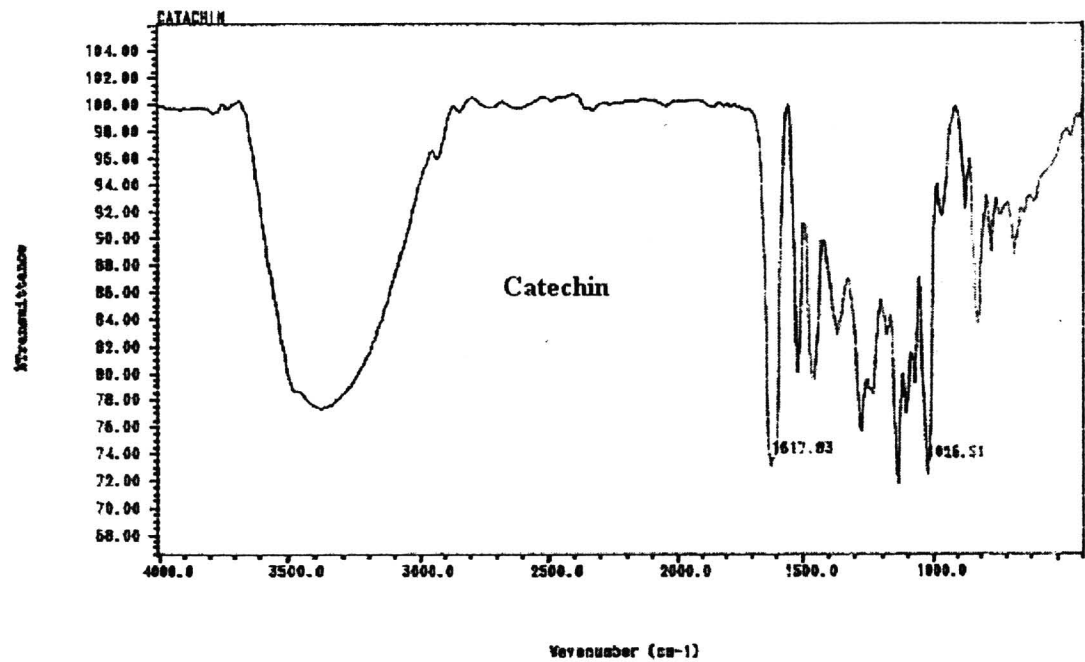


Figure 25 Infrared spectrums of catechin (flavan-3ol, proanthocyanidins) using KBr disc

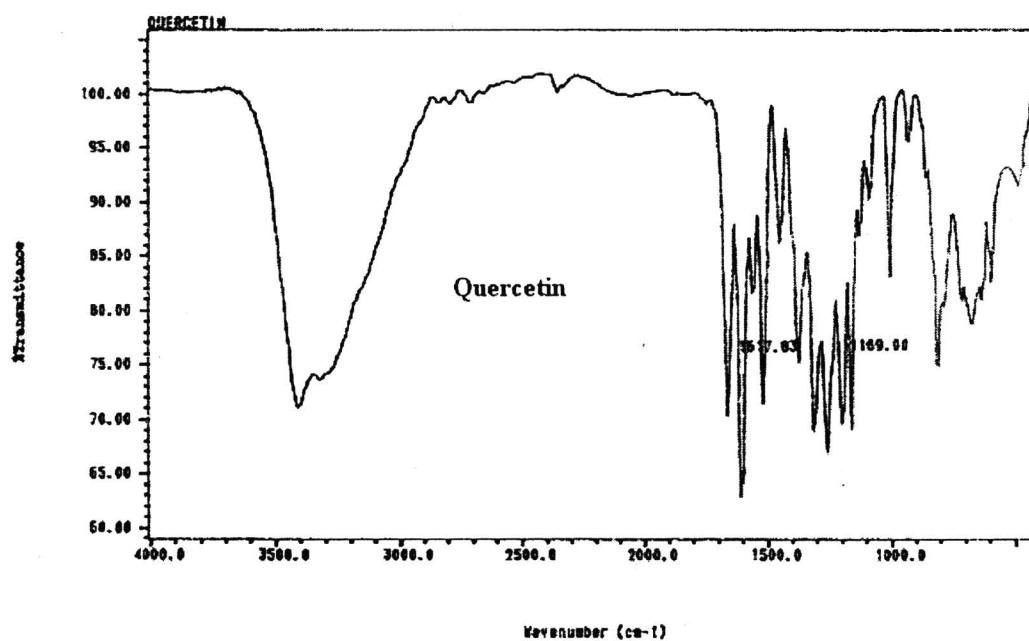


Figure 26 Infrared spectrums of quercetin (flavonols) using KBr disc

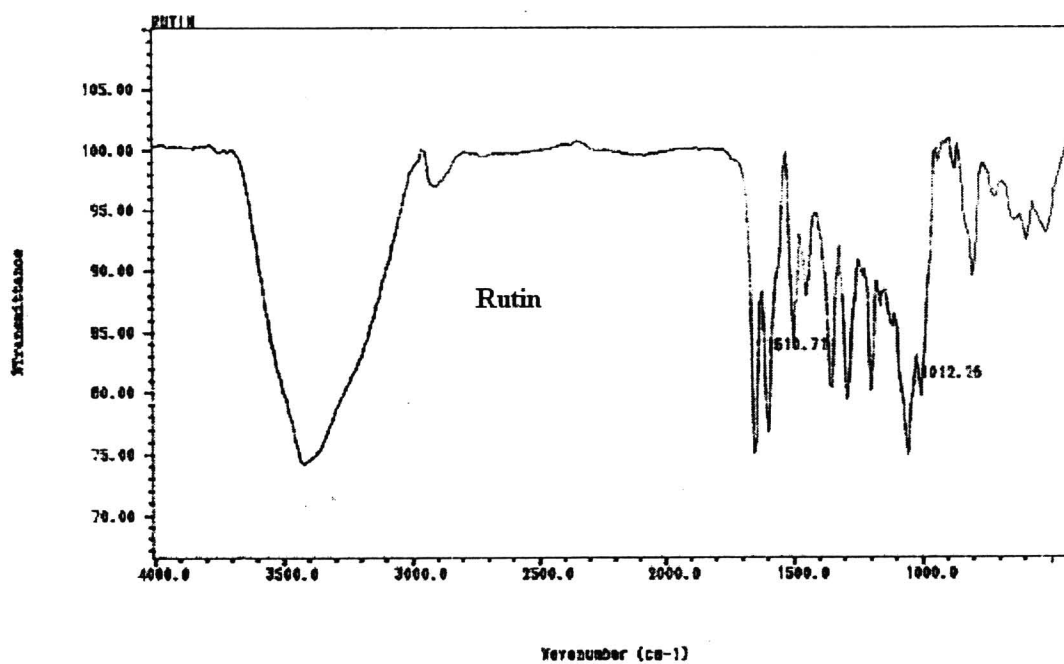


Figure 27 Infrared spectrums of rutin (flavonol glycoside) using KBr disc

The only difference between the IR spectrum of TA (Figure 20) and aTAS (Figure 23) was the disappearance of carbonyl group at $1,685\text{ cm}^{-1}$. The carbonyl group was found in galloyl group or flavonols (quercetin in Figure 26 and rutin in Figure 27). However, this carbonyl group was not found in flavan-3-ol (proanthocyanidins) such as catechin (Figure 25). The hydrolysate of aTAS (Figure 24) had the similar IR spectrum comparing with aTAS (Figure 23).

2. HPLC profiles of polyphenols in TA, aTAS, and hydrolysed aTAS

The reversed phase HPLC using eluting solvent system 1 (in chapter 3) was used to determine the phenolic compounds in TA and aTAS comparing with GSE. The several small peaks (at 14.55, 15.23 and after 30 min) and one wide peak (between 18-30 min) were found in the native TA (Figure 28). This wide peak should be the peaks of condensed tannin which contains various kinds of proanthocyanidins species in different isomer, branching and number of subunit.

The TA, aTAS and GSE were hydrolysed by hydrochloric acid refluxed in methanol. The HPLC profile of TA hydrolysate (Figure 29) was almost identical with the GSE hydrolysate (Figure 30). The presence of many isomers of flavonoids with similar polarity, results in overlapping retention time. Each peak from HPLC chromatogram of hydrolysate may be the monomers of flavonoids or their derivatives which found after hydrolysis of condensed tannin in TA (Figure 29) or GSE (Figure 30).

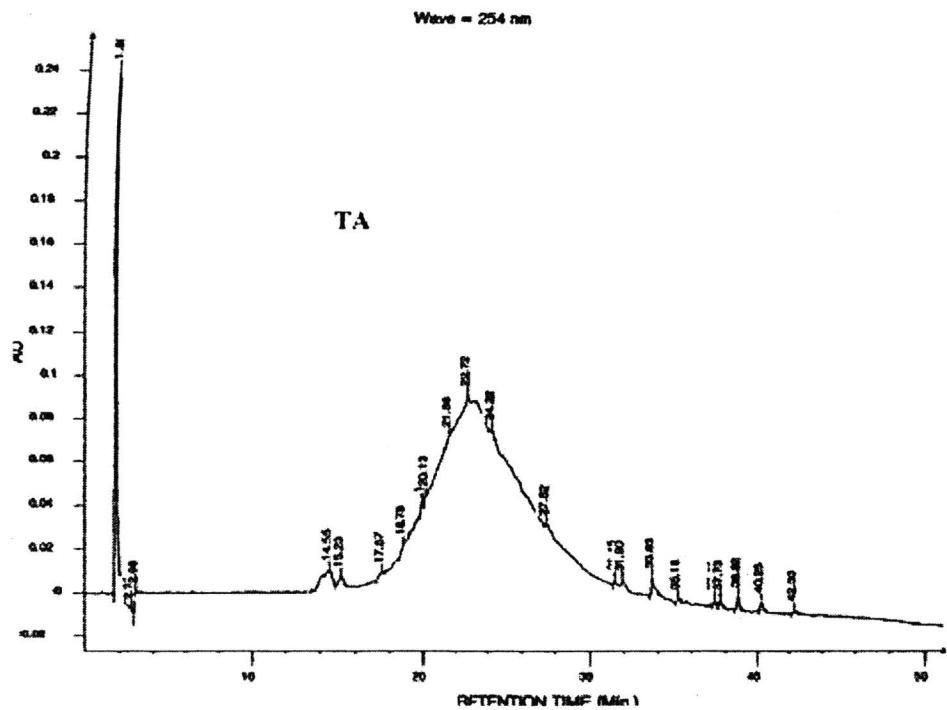


Figure 28 HPLC chromatogram of TA using gradient of 2% acetic acid and acetonitrile as mobile phase

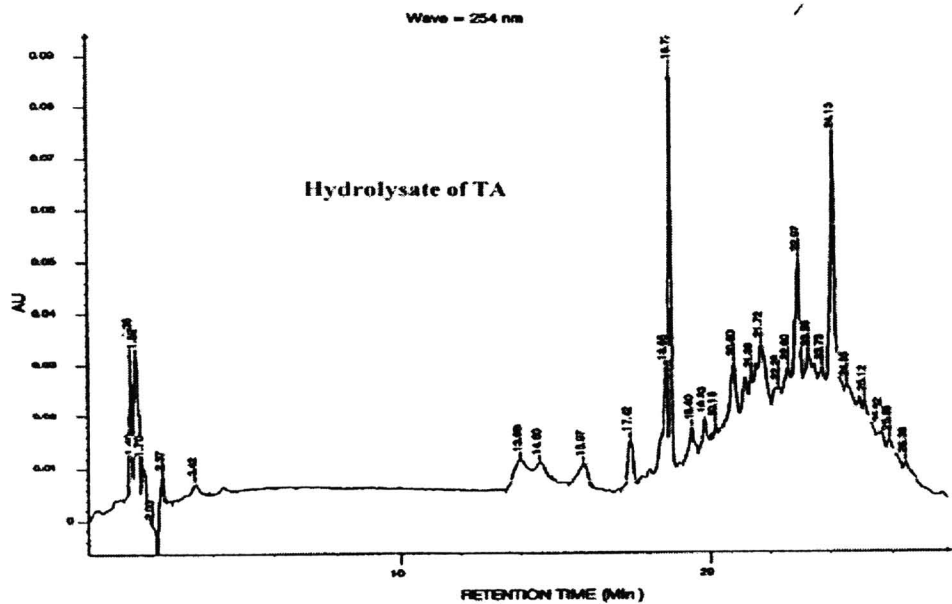


Figure 29 HPLC chromatogram of TA hydrolysate using gradient of 2% acetic acid and acetonitrile as mobile phase. More detailed data of the characteristics are shown in Table 16 (Appendix B).

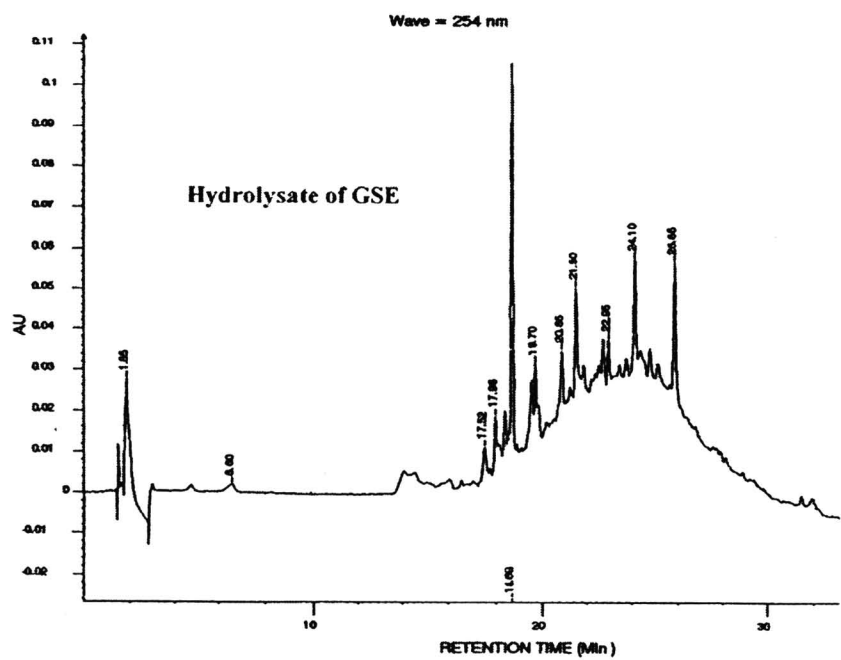


Figure 30 HPLC chromatogram of GSE hydrolysate using gradient of 2% acetic acid and acetonitrile as mobile phase. More detailed data of the characteristics are shown in Table 17 (Appendix B).

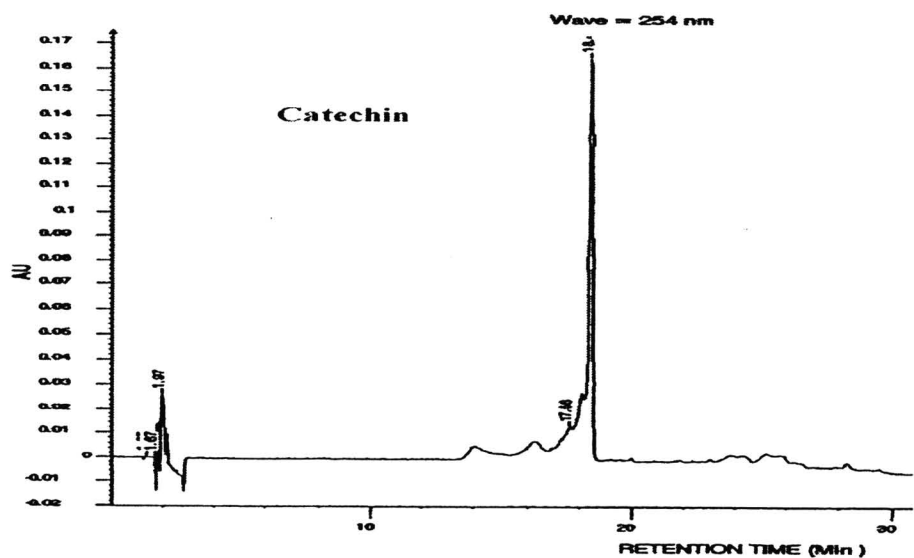


Figure 31 HPLC chromatogram of catechin using gradient of 2% acetic acid and acetonitrile as mobile phase. More detailed data of the characteristics are shown in Table 18 (Appendix B).

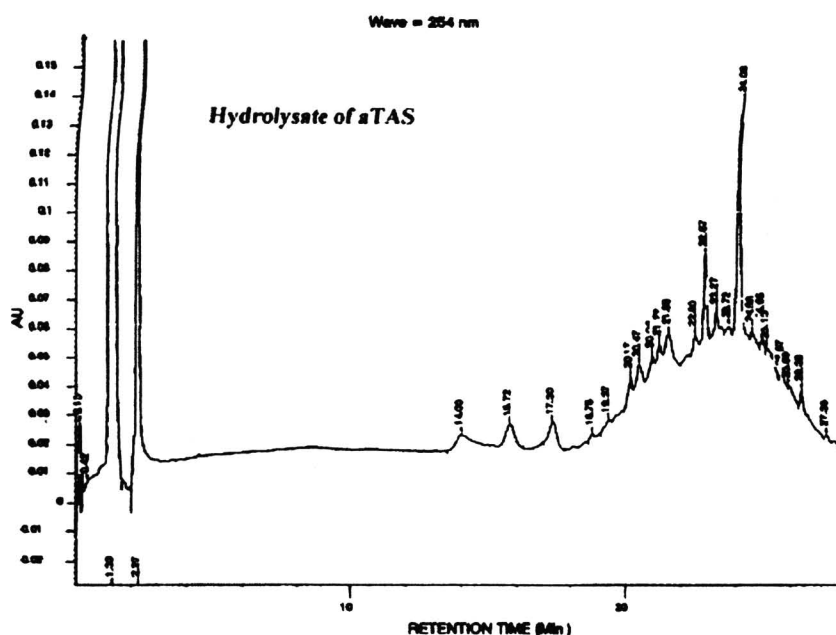


Figure 32 HPLC chromatogram of aTAS hydrolysate using gradient of 2% acetic acid and acetonitrile as mobile phase. More detailed data of the characteristics are shown in Table 20 (Appendix B).

The highest peak of HPLC chromatogram of hydrolyzed TA at 18.72 minutes was identified as catechin (Figure 31). Although the relative peak of catechin in TA (Figure 28) was not clear, it was clearly observed after hydrolyzing TA (Figure 29). However the HPLC chromatogram of aTAS hydrolysate didn't show the high content of catechin (Figure 32).

Antioxidant activities of flavonoids from TA and their mechanisms

1. Antioxidant activity of flavonoids in TA and its fractions by ABTS method

For ABTS/ metmyoglobin/ H_2O_2 method, antioxidative activity was calculated as Trolox equivalent antioxidant activity (TEAC) per 1 mg of the substance. The young TaSH exhibited greater antioxidant potentials when compared with the mature TaSH (Table 7). The husk from young seeds was difficult to separate from the seeds. The difference in color between young TaSH (green) and mature TaSH

(brown) may indicate their different compounds (Figure 33). In this study, the mature TaSH were used because they were found abundant as waste product from fruits industry and easily separated from seeds.

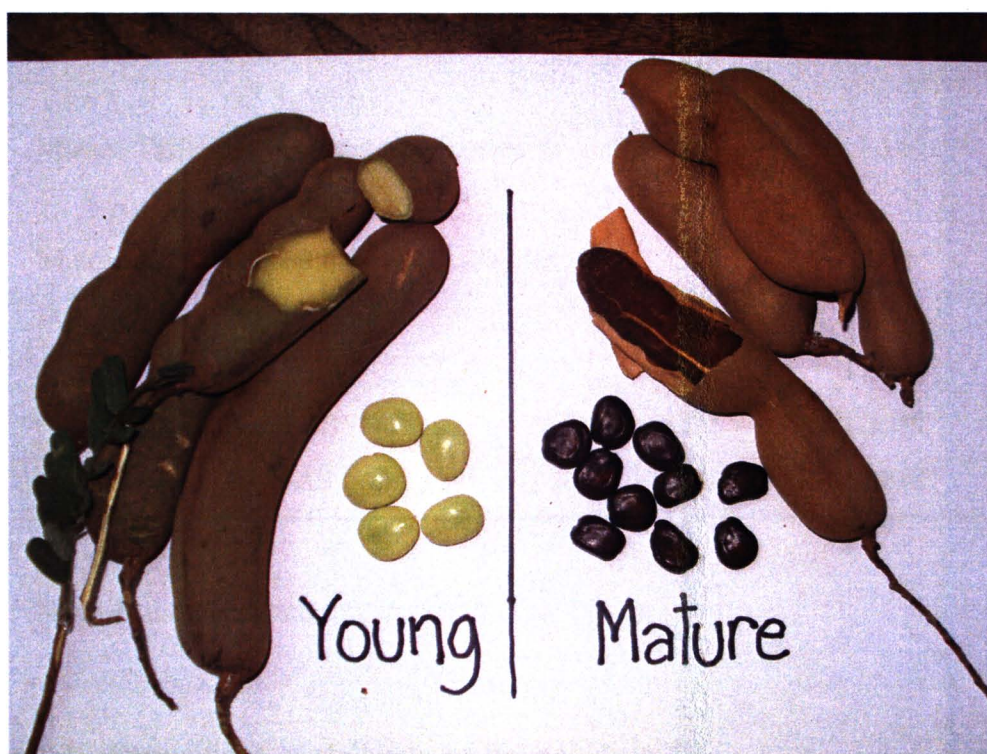


Figure 33 Young tamarind fruits and their seeds compared with mature tamarind fruits and their seeds showing different colors.

Antioxidative activities of TA were chemically assessed by determining their direct inhibition of scavenging activity by ABTS and DPPH method. The young TaSH exhibited greater antioxidant potentials when compared with the mature TaSH (Table 7). The mature TaSH extracted by acetone/water (7:3, v/v) (TA) revealed the higher content and antioxidant activity comparing with that extracted by ethanol/water (7:3, v/v). TEAC was used to assess the antioxidant potential of TA and its fractions with the following order of potency: aTAS > mTAS > TA > eTAS (Table 7).

Table 7 TEAC of the different TaSH extraction and TA fractions (eTAS, mTAS and aTAS) using ABTS/ metmyoglobin/ H₂O₂ method.

Samples	Yield (%)	TEAC
Young TaSH extracted by ethanol/ water (7:3, v/v)	ND	0.812
Mature TaSH extracted by acetone/water (7:3, v/v) (TA)	35	1.14
Mature TaSH extracted by ethanol/water (7:3, v/v)	28	0.711
eTAS	ND	1.0927
mTAS	ND	1.3549
aTAS	ND	1.3858

Note: ND = Not determined

2. Antioxidant mechanisms of flavonoids in TA

The time course of ABTS radical formation in the presence of the various concentration of TA is shown in Figure 34. The TA induces a lag time in the accumulation of ABTS radicals proportional to the concentration of the TA used. So the antioxidative mechanism of TA was the radical scavenging mechanism. The TA also induces a concentration-dependent decrease in rate of ABTS radical formation, since the rate after lag phase is lower than that of control. From these results, another mechanism of TA was the inhibitor of free radicals formation.

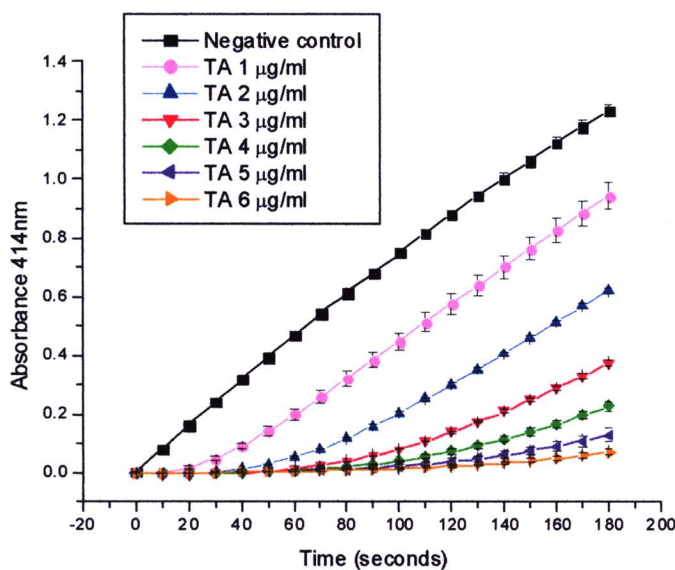


Figure 34 Kinetic reaction and dependence of antioxidant activity on concentrations of the acetone extract (TA) as determined by ABTS/metmyoglobin/H₂O₂ method.

The antioxidative action of TA was confirmed using post addition assay. The kinetic reaction was measured by ABTS/metmyoglobin/ H₂O₂ reaction starting with a negative control and then TA was added at the time of 90 second (Figure 35). The slope was changed due to the TA addition; therefore the antioxidant in TA was proved to be the inhibitor of free radical formation. Addition of TA also decreases the absorbance, caused by scavenging of ABTS radicals. It has been concluded that TA displays the mix action of scavenger and inhibitory effects on free radicals.

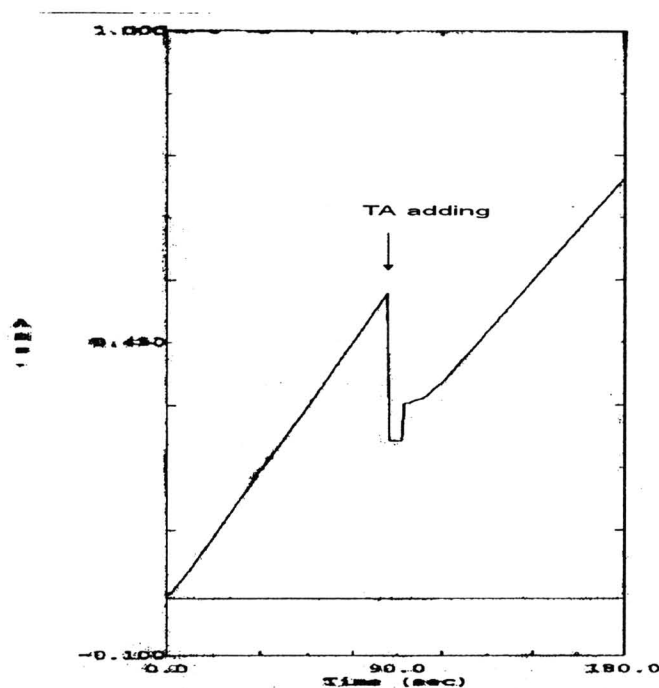


Figure 35 The graph of ABTS radical formation after post-addition with TA.

The reaction between metmyoglobin, ABTS and H_2O_2 was allowed to proceed until the colour was stable (absorbance reached 0.5), then decolorization was initiated by the addition of TA (5 $\mu\text{g}/\text{ml}$).

3. Antioxidant activity of flavonoids in TA and its fractions by DPPH method

DPPH is a radical with a strong absorption band at 517nm. When this compound accepts an electron from an antioxidant to become more stable the absorption at 517 was lost. The TA ($\text{IC}_{50} = 18 \mu\text{g}/\text{ml}$) attenuated the stable free radical of DPPH in a dose-dependent manner and acted as a more potent radical scavenger than Trolox ($\text{IC}_{50} = 28 \mu\text{g}/\text{ml}$). The radical scavenging activity of aTAS was higher than mTAS and eTAS, respectively (Figure 36).

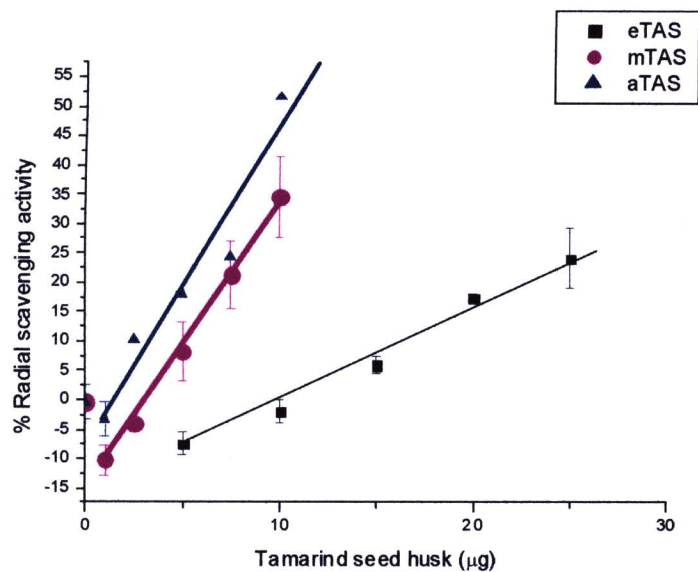


Figure 36 %Radical scavenging activity of eTAS, mTAS and aTAS using DPPH method

Chelation and enhancing autooxidation of iron by TA flavonoids

The UV-VIS spectrums of TA showed the band I at 450 nm and band II at 280 nm, which were related to B and A ring of flavonoids, respectively (Figure 38). In the UV range the spectrum of TA, after adding with ferric ions, shifted from 280 nm to 294.4 nm. The bathochromic shift band at 294.4 nm increased by dose dependent of ferric ions (Figure 37). In the visible range, the spectrum of TA after adding ferric ions shifted from 480 nm to 582 nm in a dose dependent manner (Figure 38). The absorbance at 582 nm also increased in a dose-dependent of ferric ions (Figure 39).

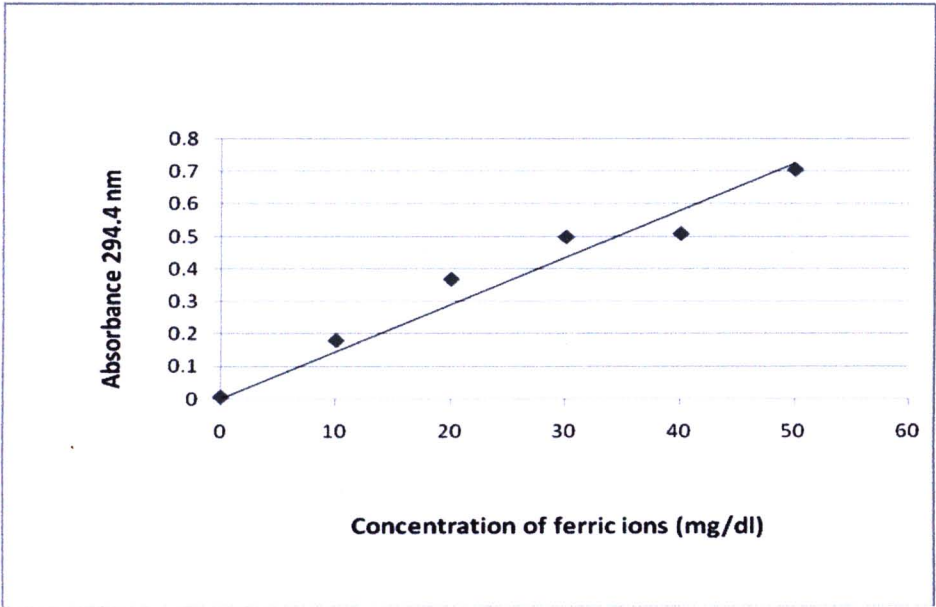


Figure 37 The absorbance of bathochromic shift band at 294.4 nm increased by dose-dependence of ferric ions.

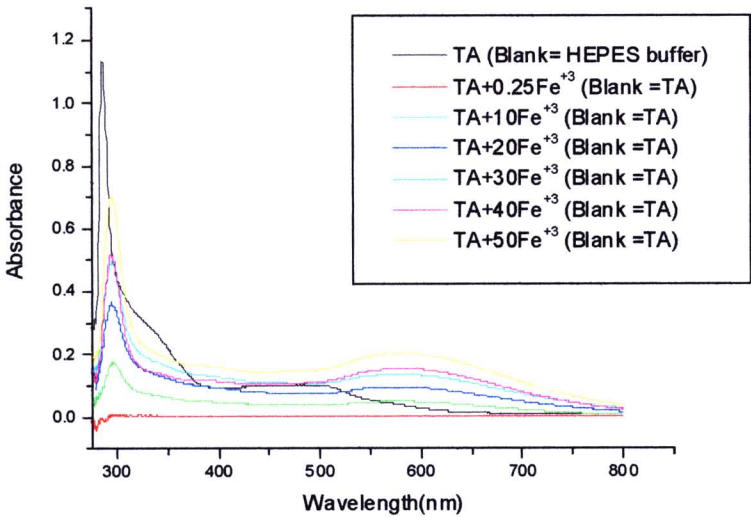


Figure 38 UV-VIS Spectrum of TA (final concentration 100µg/ml) and TA with various concentrations of ferric ions from 0.25-50 mg/dl (using TA as blank).

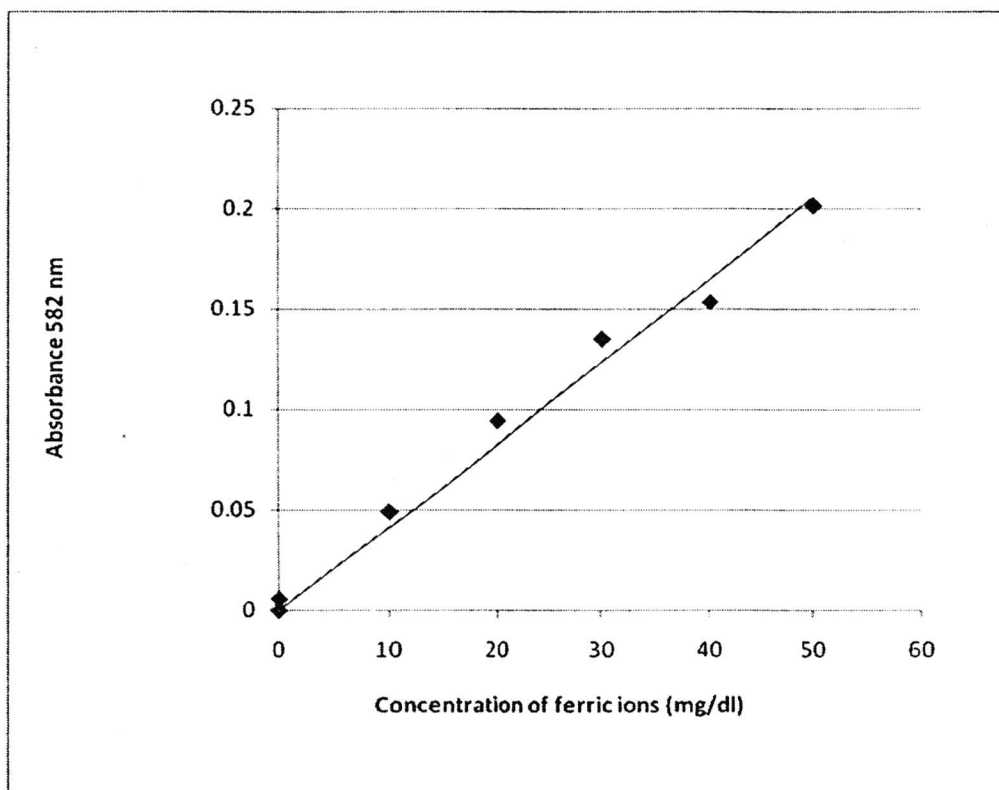


Figure 39 Absorbance of bathochromic shift band at 582 nm increased by dose-dependence of ferric ions.

In the next experiment, the influence of TA comparing with GSE on the redox state of iron at the physiological pH was investigated. The TA and GSE at concentration 20 $\mu\text{g/ml}$ could enhance the autooxidation of ferrous ion (Figure 40).

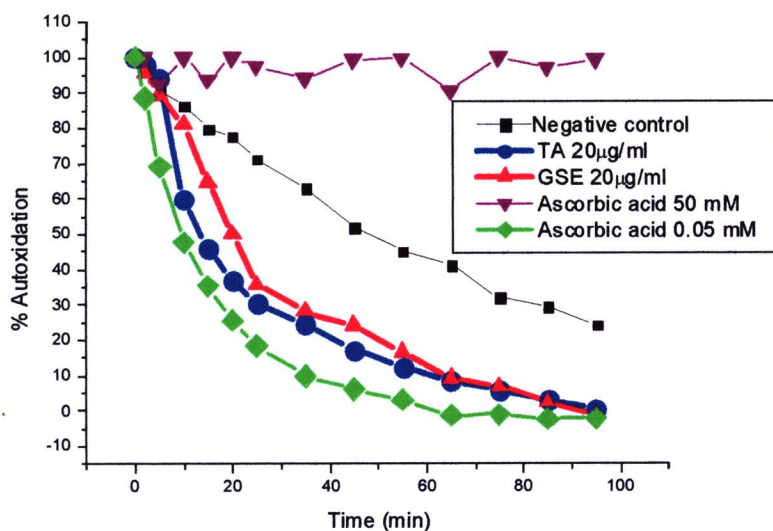


Figure 40 Increasing effects of TA and GSE on autooxidation of ferrous ion

Effects of TA flavonoids on cell viability

1. Effects of TA flavonoids on normal cell viability by neutral red method

This study demonstrated that TA interferes with the apparent viability of RGC-5 and HT-22 cells using the neutral red assay. The retina ganglion cells (RGC-5) treated with TA at various time revealed the higher absorbance of neutral red than controls in the RGC-5 cell viability (Figure 41). The percent of cell viability was calculated from the absorbance at 570 nm of sample comparing with control. The increasing effect of TA on percent RGC-5 cells survival at concentration 20 µg/ml was decreased with time dependent (Figure 42). This increasing effect on RGC-5 cell survival was found not only in TA but also found in the fraction of TA (eTAS, mTAS and aTAS) from Sephadex LH20 (Figure 43).

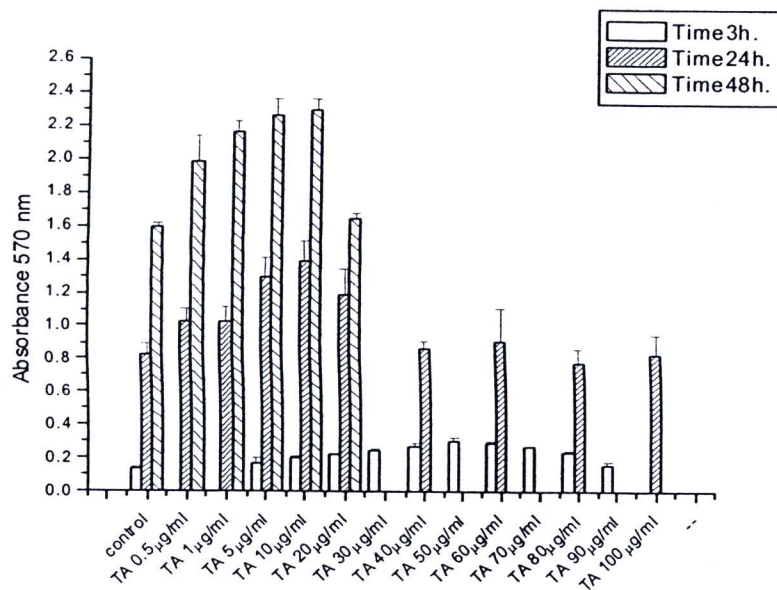


Figure 41 Increasing absorbance at 570 nm of neutral red effect in RGC-5 cell viability method after added with various concentration of TA at 3, 24 and 48 hours. Each shown value represents the mean \pm SD of four different samples.

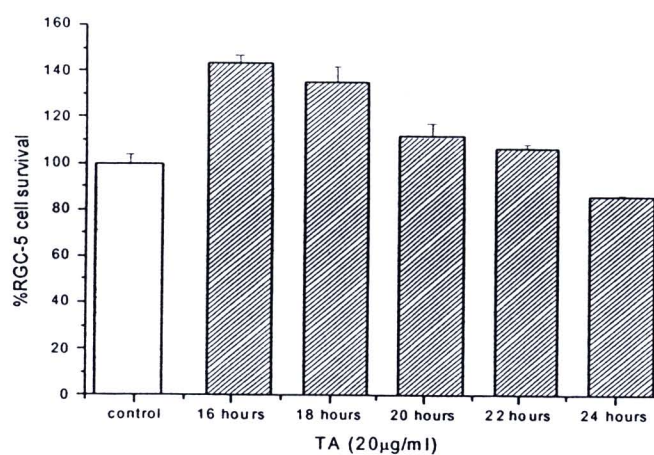


Figure 42 Cell viability response of retinal ganglion cells (RGC-5) exposed to TA at different treatment period. Each shown value represents the mean \pm SD of four different samples.

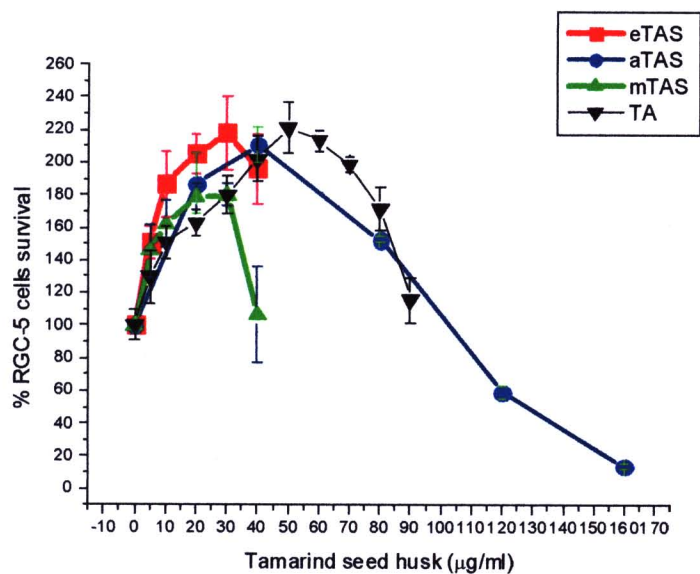


Figure 43 Increasing effects of eTAS, aTAS and mTAS on RGC-5 cells survival incubation for 3 hours. Each shown value represents the mean \pm SD of four different samples.

Instead of RGC-5, the viability of hippocampal ganglion cells (HT-22) exposed to TA at different concentrations was performed. The HT-22 cultured cells were growing in DMEM medium with 10% fetal bovine serum and 1% penicillin and streptomycin. Fetal bovine serum contains several kinds of proteins and growth factors which were necessary for cell proliferation. In our experiment, the serum-free medium changed, instead of normal medium, after addition of TA. In a serum-free medium condition, the cell growth stopped at Go- phase with no proliferation. Interestingly, the percent of cell survival in the serum-free condition after addition of TA was still higher than control (Figure 44). The increasing effect of TA on cell survival was not due to cell proliferation. The increasing effect of TA on HT-22 cell survival was also found after adding quercetin and catechin (Figure 45).

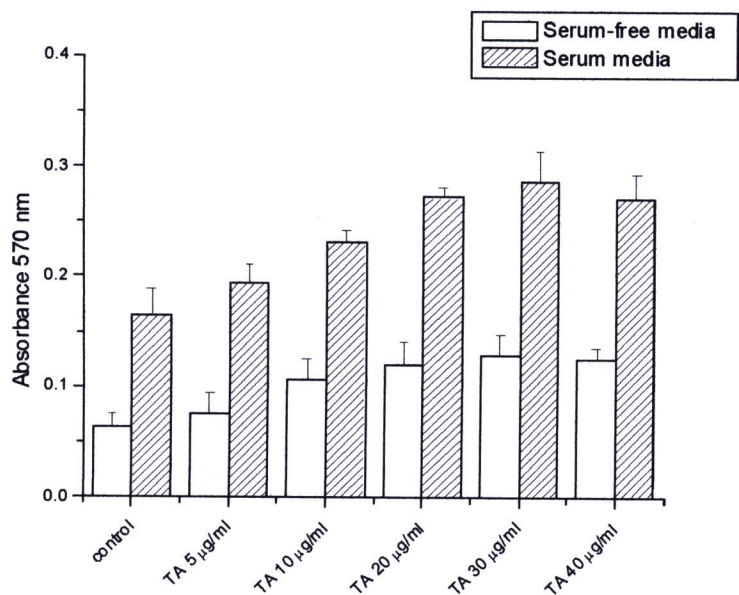


Figure 44 Hippocampal (HT-22) cells viability of TA at difference concentration in media with and without serum were determined using absorbance at 570 nm of neutral red. Each shown value represents the mean \pm SD of four different samples.

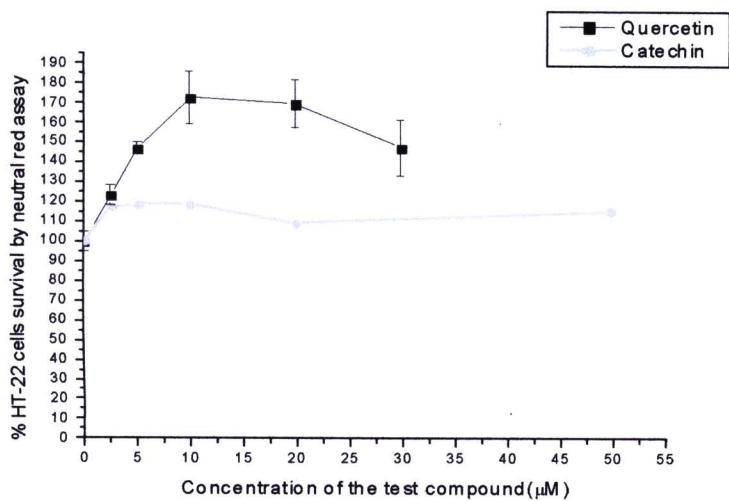


Figure 45 Cell viability response of hippocampal ganglion cells (HT-22) exposed to quercetin and catechin (as standard flavonoids)

2. Cytotoxicity of TA flavonoids on cancer cells using MTT assay

The cleavage of the soluble yellow tetrazolium salt MTT into an insoluble blue colored formazan by the mitochondrial enzyme succinate dehydrogenase is the principle of MTT assay. Absorbance at 570nm was used. The two kinds of cancer cells were used in this study; the GLC4 human small lung carcinoma cells line (GS cells) and the K562 human erythromyelogenous leukemia cells line (KS cells). In cancer cells using MTT assay to determine cell survival, the low concentration of TA (<10µg/ml) seem to increase % cells survival in both kinds of cancer cells (KS and GS cells) making no precision result after 72 hours incubation (Figure 46). However, the high concentrations of TA can calculate the IC₅₀ of TA comparing with tannic acid (hydrolysable tannins) as shown in Table 11. TA had weaker cytotoxicity effects on both cancer cells than tannic acid.

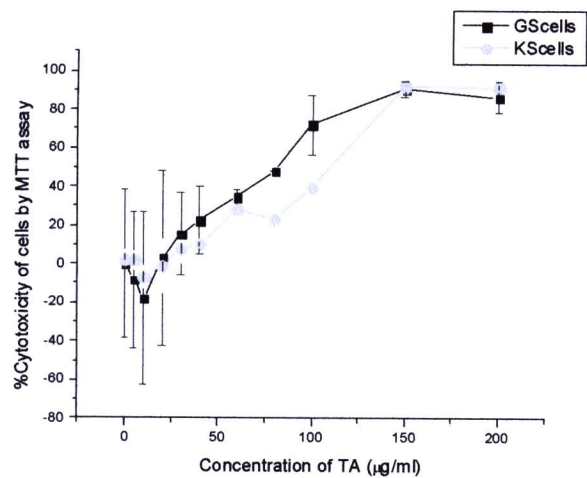


Figure 46 Cytotoxic responded of polyphenols from TA on the GLC4 human small lung carcinoma cells line (GS) and the K562 human erythromyelogenous leukemia cells line (KS cells). The cells plated into 24-wells microtitter plate in 1640 medium supplemented with 10% (v/v) fetal calf serum. The cells viability was assessed at 72 hours after adding TA using MTT assay. Each value represents the mean ± SE of three different samples.

Table 8 IC₅₀ of TA comparing with tannic acid on the GLC4 human small lung carcinoma cells line (GS cells) and the K562 human erythromyelogenous leukemia cells line (KS cells)

	IC ₅₀ of GS cells	IC ₅₀ of KS cells
Tannic acid (μg)	69.17	49.12
TA (μg)	81.92	91.15

Preparation of small molecular weight polyphenols from TA

1. Purification of small molecular weight polyphenols from TA

The partial purification using silica gel G60 quick column chromatography was used to prepare fractions. The eluting solvents were hexane, dichloromethane, ethyl acetate, ethyl acetate with acetone (4:1, v/v), ethyl acetate with acetone (1:1, v/v), acetone and methanol, respectively. The percent yield of the fractions eluting with hexane and dichloromethane was very low and couldn't be used for the further experiment. The percent yields of all the fractions of TA from silica gel was only 16.6% of TA (Table 8), while many compounds still remain in the top of silica gel. Since percent yield of TA was about 35% of TaSH (Table 7), percent yield of all TA fractions from silica gel was about 5.81% of TaSH.

The fractions eluting with acetone and methanol were named as aTAQ and mTAQ, respectively. The acetone fraction (aTAQ) had higher antioxidant activity than the methanol fraction (mTAQ), ethyl acetate fraction, ethyl acetate with acetone (4:1, v/v) and ethyl acetate with acetone (1:1, v/v), respectively (Table 8). The aTAQ and mTAQ which have high antioxidant activity were collected for further experiments.

Table 9 Yield, antioxidant activity and polyphenols content of the TA fractions from silica gel chromatography with different solvents.

Solvent used	%Yield ^a of the fractions	Antioxidant activity ^b IC ₅₀ (µg/ml)	Polyphenols content (mg of GAE ^c /mg of sample)
Hexane	None	ND	ND
Dichloromethane	Very low	ND	ND
Ethyl actate	0.8	15.9 ± 0.2	ND
Ethyl acetate/acetone (4:1, v/v)	1.7	58.0 ± 1.1	ND
Ethyl acetate/acetone (1:1, v/v)	0.5	>200	ND
Acetone (aTAQ ^d)	4.3	5.5 ± 0.1	0.54 ± 0.03
Methanol (mTAQ ^e)	9.3	6.5 ± 0.2	0.34 ± 0.04

Note: ^a[dry weight of each fraction/ dry weight of tamarind seed husk extract]×100. ^bDPPH radical scavenging activity. ^cGallic acid equivalent. ^{d,e}Fractions eluted with acetone and methanol were named aTAQ and mTAQ in the text, respectively. ND= not determined. The data represented are mean ± SD.

aTAQ and mTAQ contained a high amount of polyphenols which may be related to the strong DPPH radical scavenging activity. The content of polyphenols and the IC₅₀ value for DPPH radical scavenging activity in the TA was 0.41±0.03 mg of gallic acid equivalent/ mg of the extract. The gallic acid equivalent using the Folin method were ordered as aTAQ (0.54+0.03) > TA (0.41+0.03) > mTAQ (0.34+0.04), respectively. The polyphenols content in aTAQ was increased from TA. mTAQ had the lowest content of polyphenols comparing with aTAQ and TA.

2. HPLC profiles of polyphenols from TA, aTAQ and mTAQ

The reversed phase HPLC method eluting with solvent system 2 was developed to chromatographic fingerprint of TA and its fractions comparing with GSE and pine bark extract (PBE). The retention time of standard polyphenols were listed in Table 9. However, the HPLC profiles of some standard polyphenols contained more than one peak due to their impurity (Table 9).

Table 10 HPLC retention time of standard flavonoids using gradient of 3% acetic acid and methanol as mobile phase (see Figures 72-83 in Appendix G)

Phenolic substance	Type of phenolic compounds	Retention time (min)
Gallic acid	Hydrolysable tannin derivatives, non-flavonoids	6.619, 7.53*
Ellagic acid	Hydrolysable tannin derivatives	34.389*, 52.647, 54.889
Ferulic acid	Non-flavonoid	29.184*, 52.286, 54.407
Catechin	Flavan-3-ol, procyanidin	18.718, 19.223*, 53.194
Epigallocatechin gallate (EGCG)	Flavan-3-ol, prodelphinidin	22.440, 22.769*, 25.080, 26.614
Epicatechin	Flavan-3-ol, procyanidin	23.002, 23.281*
Gallocatechin gallate (GCG)	Flavan-3-ol, prodelphinidin	24.550, 24.851*, 52.429, 53.505
Epicatechin gallate (ECG)	Flavan-3-ol, procyanidin	26.169, 26.437*, 52.478, 54.670
Catechin gallate (CG)	Flavan-3-ol, procyanidin	28.223
Rutin	Flavonol glycoside	33.071*, 53.288, 55.141
Quercetin	Flavonol	39.100*, 52.489, 54.718

Note: *The highest peak of HPLC profile.

The TA contained many phenolic compounds as shown in their HPLC profiles (Figure 47). The peak of TA at retention time 19.967 min was similar to catechin (19.223). The profile of phenolic compounds from TA (Figure 47) in both native form and hydrolysable form (see in Figure 84-88, Appendix G) was similar to that of oligomeric proanthocyanidins from GSE (Figure 48) and pine bark extract (PBE) (Figure 51). After purification by silica gel column chromatography, the acetone fraction (aTAQ) contained all main peaks in TA, while some minor peaks disappeared (Figure 49). For the methanol fraction (mTAQ), the several peaks which were found before 25 min disappeared (Figure 50). There were also many spots with long tails of antioxidant compounds on TLC plate in both aTAQ and mTAQ (data not shown).

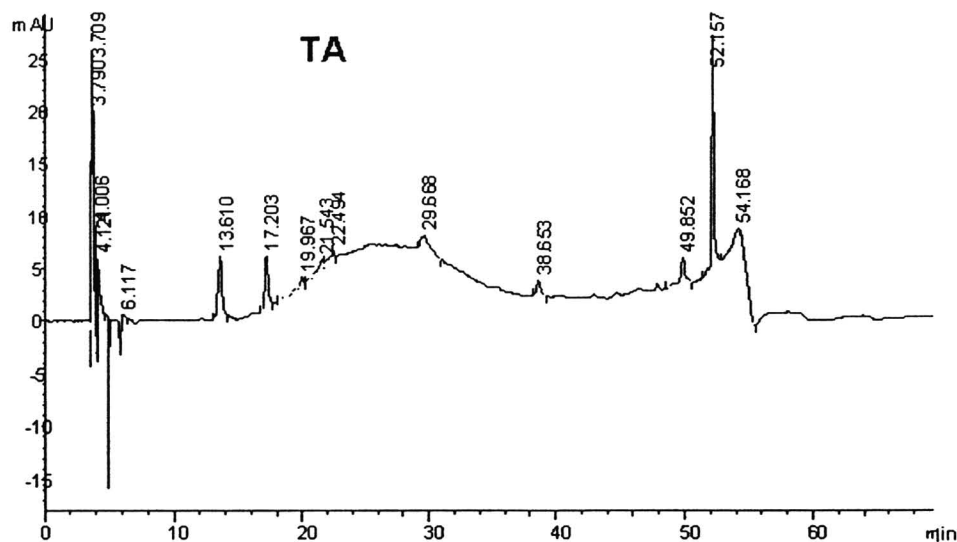


Figure 47 HPLC profiles of polyphenols from TA using gradient of 3% acetic acid and methanol as mobile phase

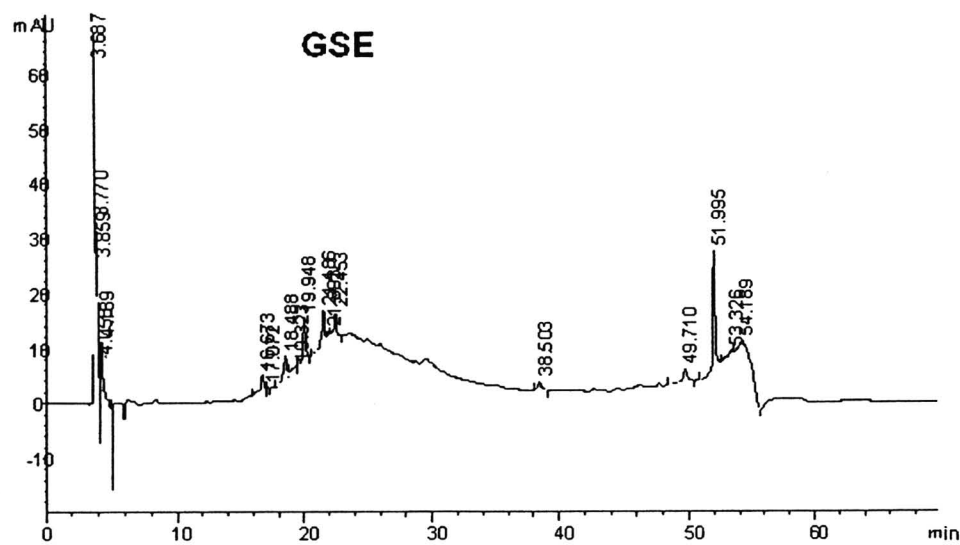


Figure 48 HPLC profiles of oligomeric proanthocyanidins from GSE using gradient of 3% acetic acid and methanol as mobile phase

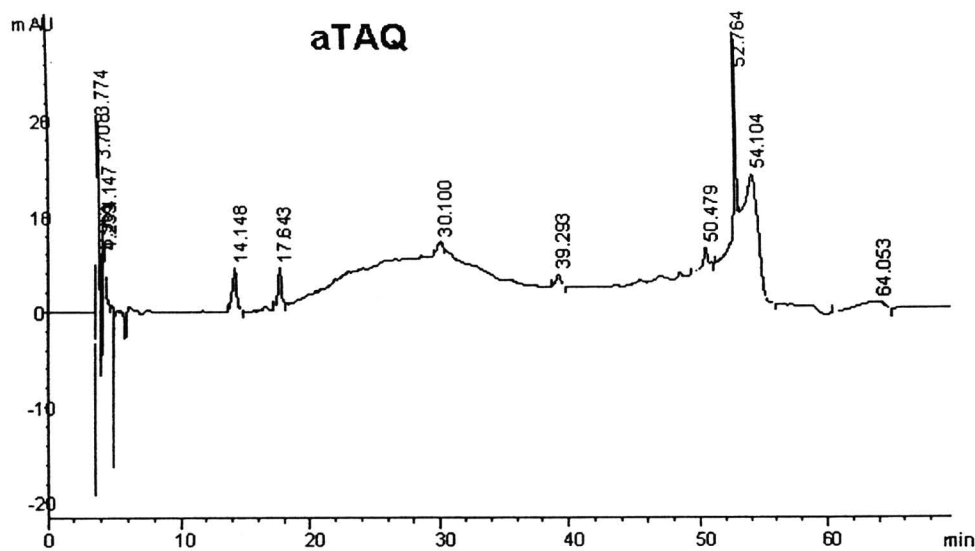


Figure 49 HPLC profiles of polyphenols from aTAQ using gradient of 3% acetic acid and methanol as mobile phase

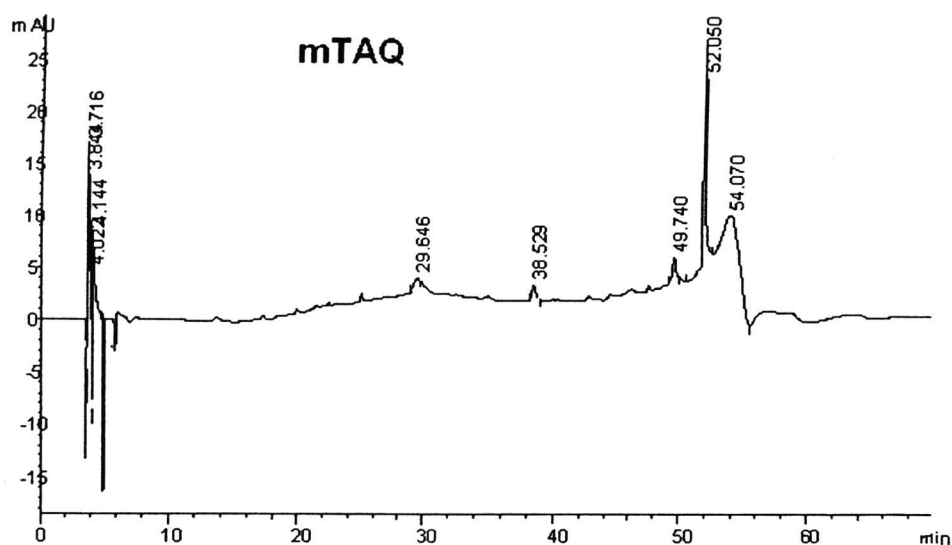


Figure 50 HPLC profiles of polyphenols from mTAQ using gradient of 3% acetic acid and methanol as mobile phase

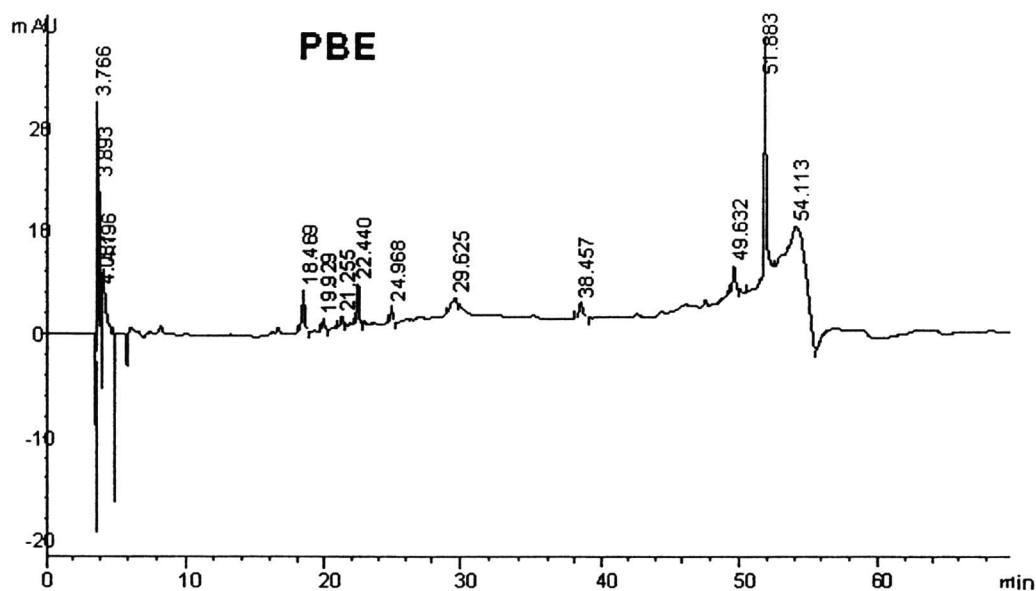


Figure 51 HPLC profiles of oligomeric proanthocyanidins from pine bark extract (PBE) using gradient of 3% acetic acid and methanol as mobile phase



Effects of small molecular weight polyphenols from TA on hemolysis and their mechanisms

1. Comparison of hemolysis induced by H₂O₂, DEM, and PHZ

The results are shown in Table 10. These three hemolytic agents show the statistically significant hemolytic effect though the hemolysis is weak due to the strong defense system of erythrocytes. The percent of hemolysis caused by DEM and PHZ in our experiment were similar to those reported by Ferrali, et al. (1992), and among these hemolytic agents, H₂O₂ were the strongest one (Table 10).

Table 11 Hemolytic effects of different oxidants and their mixture

Oxidants	% Hemolysis (Mean \pm S.E.)
Control ^a	1.7 \pm 0.1
1 mM DEM ^b	3.1 \pm 0.3 *
10 mM H ₂ O ₂	5.6 \pm 0.6 *
1mM DEM + 10 mM H ₂ O ₂	5.0 \pm 0.5 *
1mM PHZ ^c	4.1 \pm 0.3 *
1mM DEM + 1mM PHZ	4.7 \pm 0.2 *

Note: ^a No addition of oxidant. ^b diethyl maleate. ^c phenylhydrazine.

*Significant at P <0.01 vs control. Each shown value represents the mean \pm SE (n=12).

2. Inhibition of oxidant-induced hemolysis by aTAQ and mTAQ

Two kinds of partially purified polyphenols named aTAQ and mTAQ which showed the potent DPPH radical scavenging activity were obtained from TA. The IC₅₀ values of aTAQ and mTAQ for DPPH were 5.5 \pm 0.1 and 6.5 \pm 0.2 μ g/ml, respectively. Initially, no effect of aTAQ and mTAQ at the concentration of 0.5-20 μ g/ml on hemolysis was confirmed under the given experimental conditions. The percentage of human hemolysis by aTAQ and mTAQ at the concentration of 0.5-20

$\mu\text{g/ml}$ was found to be $1.6 \pm 0.1\%$ (mean \pm S.E.) which was comparable with control ($1.7 \pm 0.1\%$).

The protective effects of aTAQ and mTAQ at the final concentration of $5 \mu\text{g/ml}$ on human hemolysis caused by various oxidants were evaluated (Figure 52). aTAQ showed the remarkable inhibition of hemolysis caused by all oxidants, and mTAQ showed the weaker inhibition than aTAQ. The protective effect of aTAQ and mTAQ at low concentrations (0.5 - $5 \mu\text{g/ml}$) on human hemolysis caused by H_2O_2 alone at its final concentration of 10mM was also evaluated by dose dependent manner (Figure 53). At the high concentrations ($> 10 \mu\text{g/ml}$), the protective effects of aTAQ and mTAQ on H_2O_2 -induced hemolysis decreased (Figure 53). aTAQ showed the strong inhibition of hemolysis at $5 \mu\text{g/ml}$, and the inhibition of mTAQ was weaker than aTAQ.

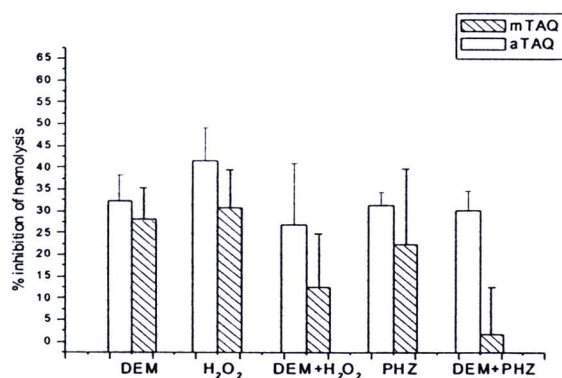


Figure 52 Inhibitory effect of aTAQ and mTAQ at concentration of $5 \mu\text{g/ml}$ on hemolysis induced by 1mM diethyl maleate (DEM), 10mM hydrogen peroxide, 1mM DEM + 10mM H_2O_2 , 1mM phenylhydrazine (PHZ), and 1mM DEM + 1mM PHZ. Each shown value represents the mean \pm SE of three different samples.

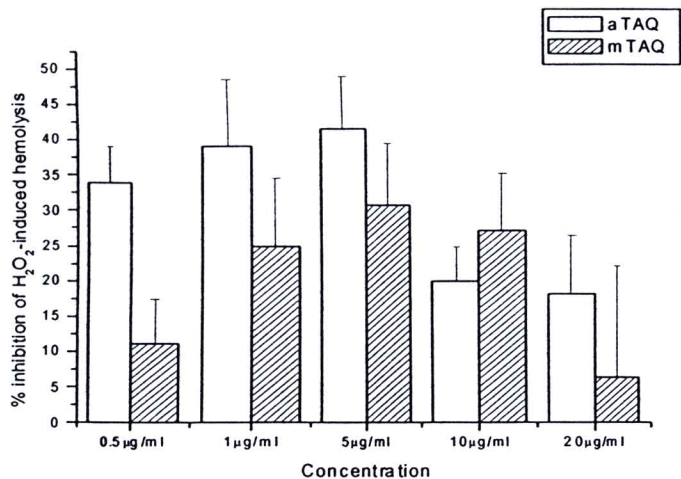


Figure 53 Effects of acetone fraction (aTAQ) and methanol fraction (mTAQ) at various concentrations in 10mM hydrogen peroxide-induced hemolysis. Each shown value represents the mean ± SE of three different samples.

3. Inhibitory effects of aTAQ and mTAQ on ROS production

As shown in Figure 54, the remarkable increase in ROS was induced by the addition of H₂O₂. aTAQ exerted a remarkable reduction of ROS even at the lower concentration of 0.1µg/ml. The dose-dependent inhibition of ROS production by aTAQ, however, was not observed, showing the similar inhibition of ROS production at 10µg/ml. The similar results were reported by Tedesco *et al.* (2000). They reported that quercetin showed strong scavenging activity for ROS production but the dose-dependence was not observed especially at higher concentration (5-20 µM). mTAQ had little or no effect on ROS production.

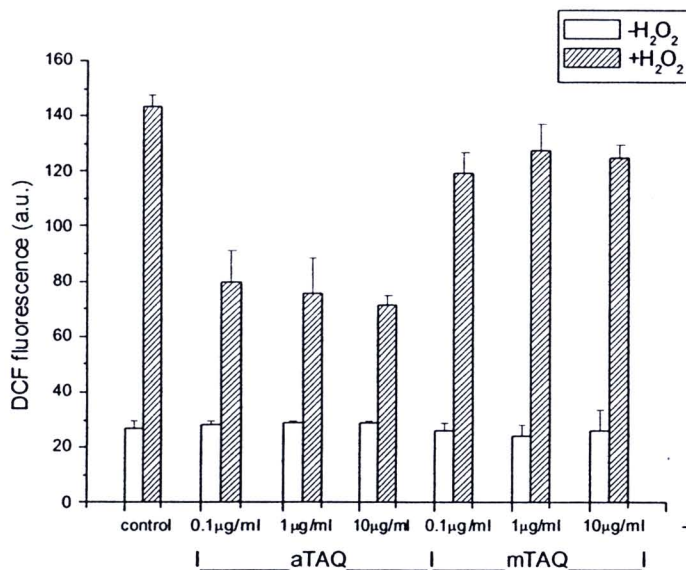


Figure 54 Reactive oxygen species (ROS) production in red blood cells pretreated with 10µl of aTAQ and mTAQ for 1 h at 37°C and incubated for 20 min with 10 mM H₂O₂. At the end of incubation, ROS production was measured as dichlorofluorescein (DCF) fluorescence. The concentrations are those in the pretreatment incubation mixtures. - H₂O₂ and +H₂O₂ mean no addition and addition of H₂O₂, respectively. For aTSE, mTSE, and the other detail, see the text. Each shown value represents the mean ± SE of three different samples.

4. Increasing effects of aTAQ and mTAQ on H₂O₂-decrease glutathione level

As shown in Figure 55, the remarkable decrease in GSH level was induced by the addition of H₂O₂. aTAQ showed the activity to inhibit H₂O₂-reduced glutathione level. But the dose-dependent activity, however, was not observed, showing the similar GSH level at 10 µg/ml of aTAQ.

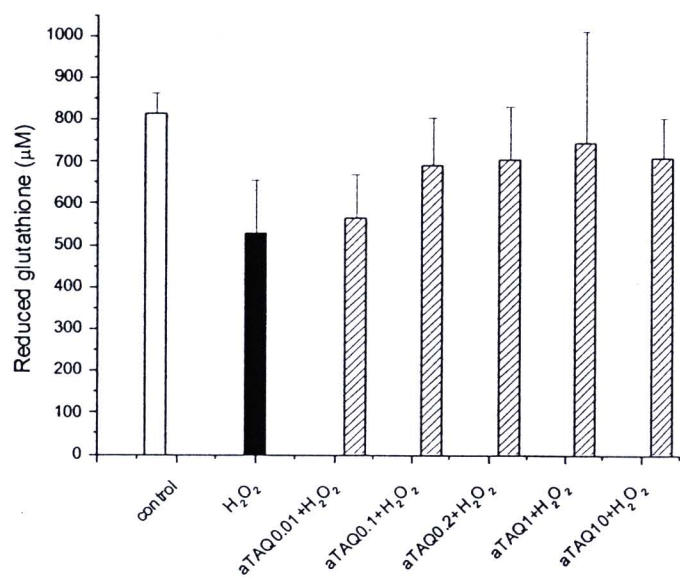


Figure 55 Inhibitory effect of aTAQ on H₂O₂-decreased glutathione (GSH) level. Each shown value represents the mean ± SE of three different samples.

5. Inhibitory effects of aTAQ on H₂O₂-induced methHb level

As shown in Figure 56, the remarkable increase in methHb was induced by the addition of H₂O₂. aTAQ showed the activity to inhibit H₂O₂-induced methHb formation even at the low concentration of 0.05 µg/ml.

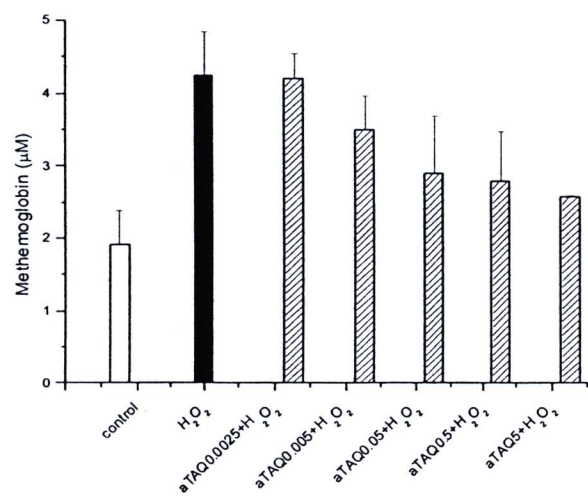


Figure 56 Inhibitory effect of aTAQ on H₂O₂-induced methemoglobin formation in red blood cells after 3 hours incubation. Each shown value represents the mean ± SE of three different samples.

Inhibitory effects of TA on oxidant-induced DNA damage

The double-stranded plasmid exists in a tightly compact supercoiled formation in its native form and as such it has a relatively high electrophoretic mobility. In DNA nicking method, when treated with an agent that induced DNA strand breaks, supercoiled DNA was converted to the open-circular (or relaxed) conformations by a single-strand break and to linear DNA by a double-strand break (Moriwaki *et al.*, 2008). Extensive double-strand breakages lead to DNA degradation. The migration pattern of a plasmid under the gel electrophoresis conditions is: supercoiled > linear > open-circular DNA.

Free radical produced by the Fenton reaction could decrease the amount of supercoiled strands of DNA and increase the damage strands of DNA in either linear strands or open-circular strands. In our experiment, the pUc18 DNA which was added with 0.1mmole H_2O_2 (6.66 mM) and 0.024 μmole FeSO_4 (1.6 μM) in big wells (15 μl) induced single strand breaks by converting supercoiled strands to open-circular strands of DNA (Figure 57). In the small well (7.5 μl), DNA adding with 0.05 mmole H_2O_2 (6.66 mM) and 0.012 μmole FeSO_4 (1.6 μM) induced double strand breaks by converting supercoiled strands to linear strands of DNA (Figure 58-59). The addition of H_2O_2 with ferrous sulfate significantly enhanced the breakage of DNA, super-coiled form DNA have been converted into circular relaxed double-strand DNA or linear strand DNA up to the content of them.

In this study, the plasmids pUc18 DNA were treated with TA at concentration of 0.1, 1, 40 100, 200 $\mu\text{g/ml}$ using Fenton conditions to induce oxidation and the treated plasmids were analyzed by agarose gel electrophoresis (Figure 57). TA could protect Fenton reactant-mediated supercoiled DNA damage by dose dependent (Figure 57). However, the inhibitory effect of TA on Fenton reactant-induced open-circular formation was not by dose dependent manner (Figure 57). Crude (TA), acetone (aTAQ) and methanol (mTAQ) fractions of tamarind seed husk (TaSH) as well as grape seed extract (GSE) can clearly inhibit Fenton reactants -induced supercoiled DNA strand scissions in both single strand and double strand scissions (Figure 57-59).

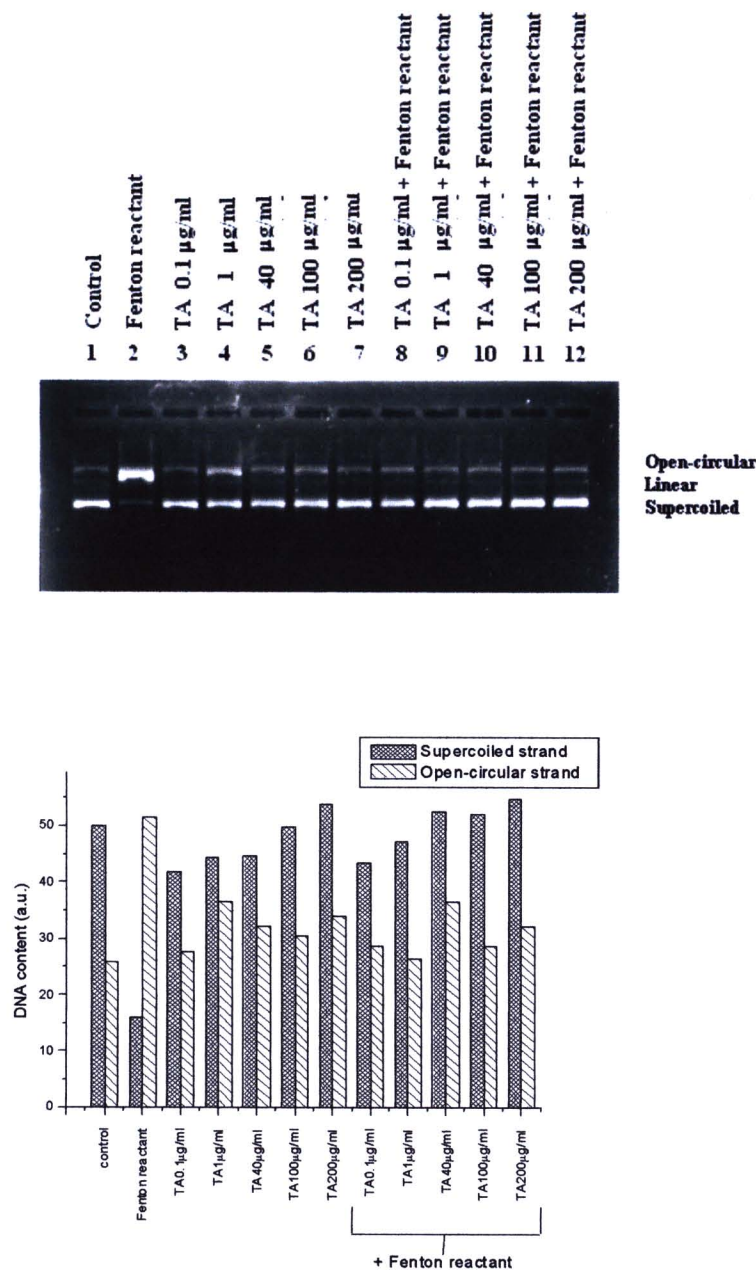


Figure 57 Inhibitory effect of TA on Fenton reactants -induced supercoiled DNA strand breakage (upper figure): (lane 1) DNA incubated without Fenton reactants; (lane 2) DNA incubated with Fenton reactants; (lane 3-7) DNA incubated with TA at 0.1, 1, 40, 100, 200 µg/ml, respectively; (lane 8-12) DNA incubated with TA at 0.1, 1, 40, 100, 200 µg/ml with Fenton reactant. Each point represents the mean ± SD of duplicate measurements (lower figure).

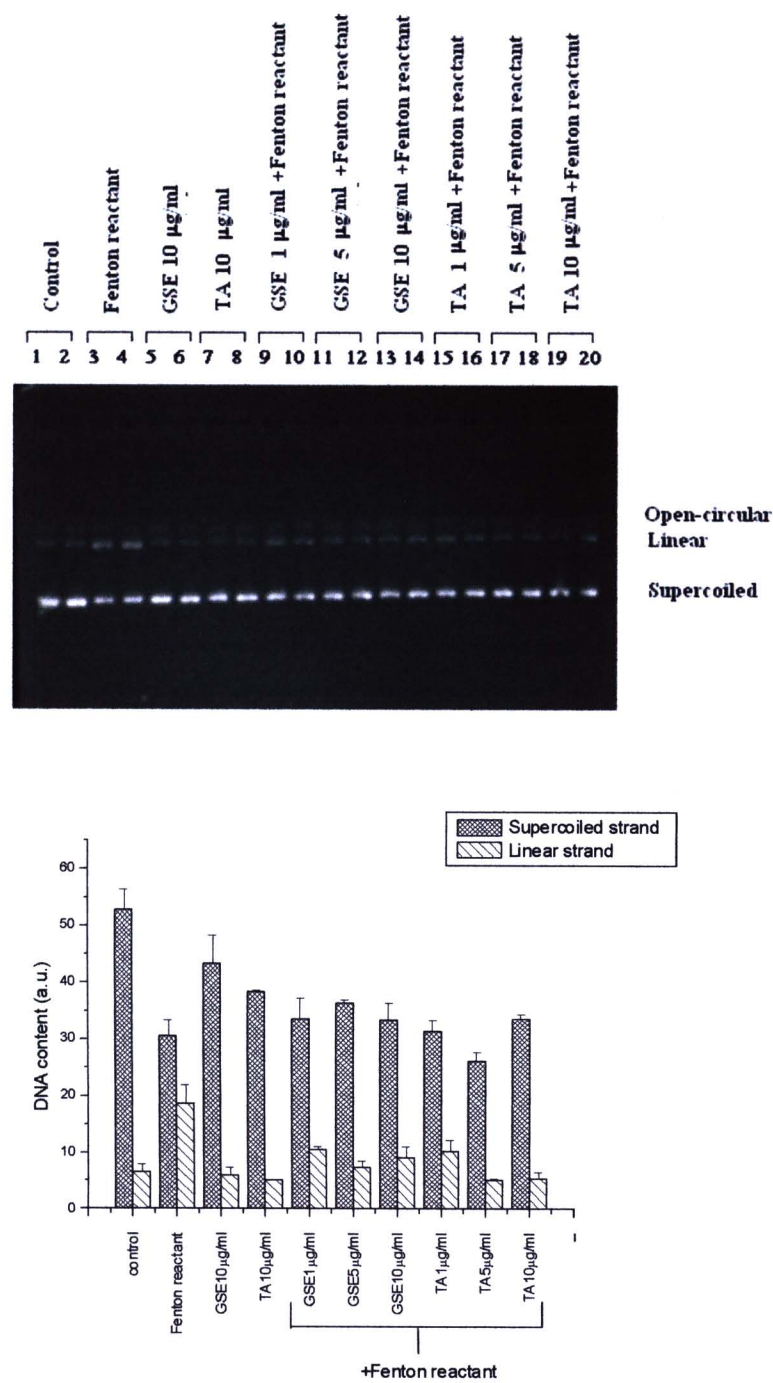


Figure 58 Effect of grape seed extract (GSE) and tamarind seed husk (TA) on Fenton reactant -catalyzed double strand breakage of plasmid pUc18 DNA (upper figure). Each point represents the mean \pm SD of duplicate measurements (lower figure). Fenton reactants are 0.05 mmole H_2O_2 (6.66 mM) and 0.012 μmole FeSO_4 (1.6 μM).

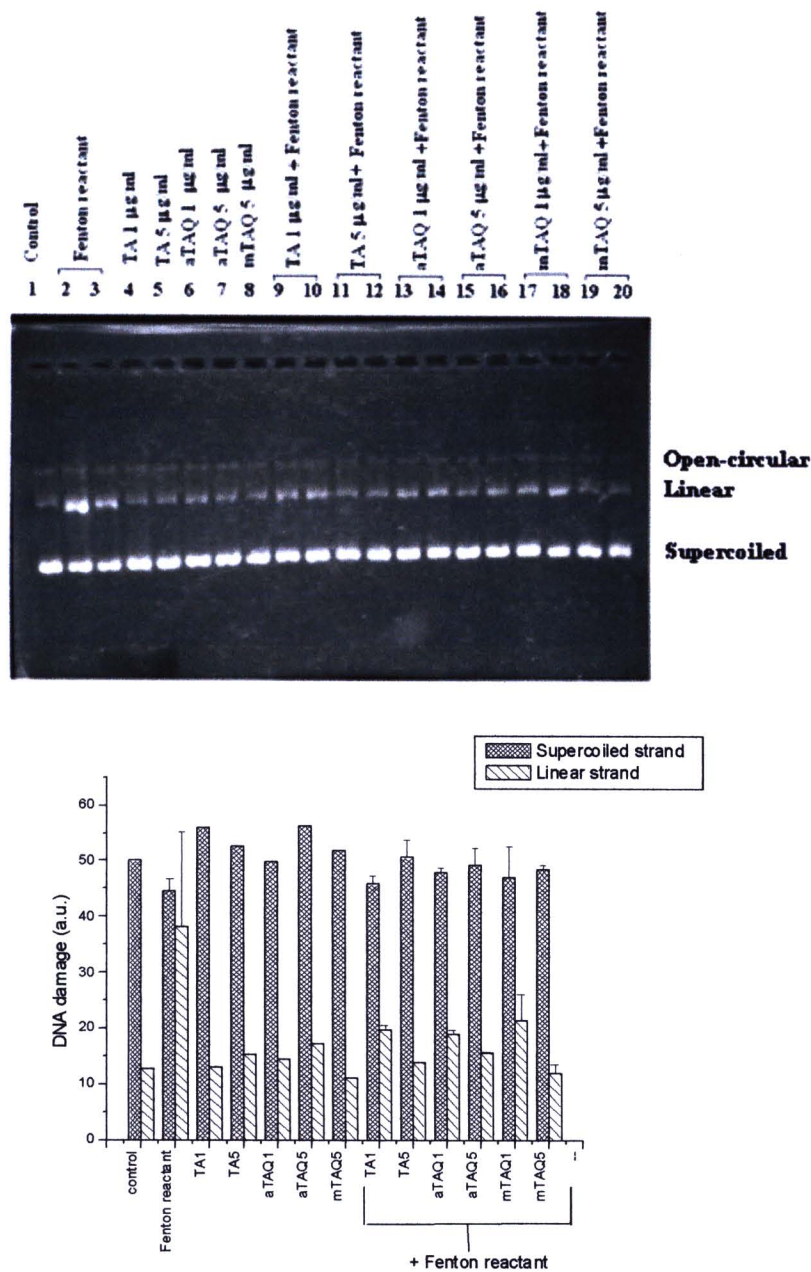


Figure 59 Inhibitory effect of tamarind seed husk extract (TA) and their fraction on Fenton oxidant-catalyzed double strand breakage of plasmid pUc18 DNA. The migration pattern of a plasmid under the gel electrophoresis conditions is: supercoiled > linear > open circular DNA (upper figure). Fenton reactants are 0.05 mmole H₂O₂ (6.66 mM) and 0.012µmole FeSO₄ (1.6 µM). Each point represents the mean ± SD of duplicate measurements (lower figure).

Preparation of polymeric proanthocyanidins from TE and GE by Sephadex LH20 column chromatography

TaSH and GS of *Vitis vinifera* cv. Ribier (Pok Dum) were extracted with ethanol/water (3:2, v/v) at 60°C for 24 hours, and the crude extracts of TaSH (TE) and the crude extract of GS (GE) were obtained. Crude extracts were further purified with Sephadex LH20 according to slightly modified method of Peng, et al. (2001). Extraction from partly dried grape seed (GS) was also carried out in the same way as TaSH.

Table 12 Yield (%) and content of polymeric proanthocyanidins (PA) in TaSH, GS, TE, and GE

	Number of extraction repetition	Yield(%) ^a	Water content (%) ^b		Content of polymeric PA (%)	
			Partly Dried material ^c	Fresh material	Extract ^d	Fresh material ^e
TE	1 ^f	43.5±2.0	-	-	94.1±0.4	-
	3 ^g	47.0±1.8	-	-	87.7±1.5	-
TaSH	-	-	14.6±0.3	18.9±0.3	-	39.1
GE	3	13.5±1.1	-	-	37.3±4.1	-
GS	-	-	8.5±0.3	42.3±1.3		3.2

Note: ^aPercentage of the extract from the partly dried material (TSH and GS) using ethanol/water (3:2 v/v) at 60 °C for 24 h. ^bdry weight loss (dried to a constant weight at 110 °C), ^cpartly dried material (see the text for drying conditions), ^dcontent of polymeric proanthocyanidins in the extract, estimated content of polymeric proanthocyanidins in the fresh TSH and GS, ^fone pot extraction, ^gthree times repeated extraction.

The contents of polymeric proanthocyanidins (PA) in TE and GE were analyzed by HPLC and determined using acTSE and acGSE as a standard. And the content of polymeric proanthocyanidins in fresh TSH and fresh GS was calculated from yield, percent of polymeric proanthocyanidins in extract, and water content of partly dried and fresh materials (TaSH and GS).

The results were summarized in Table 12. The content of polymeric proanthocyanidins in fresh TaSH reached about 39% (w/w), which was about 13 times higher than that in fresh grape seeds. The content of polymeric proanthocyanidins in TE prepared by one pot extraction with ethanol/water (3:2, v/v) at 60°C for 24 hours was very high (about 94%, w/w).

HPLC/UV analysis of polymeric proanthocyanidins from aTES and aGES

The HPLC chromatograms at the concentration of 5 mg/ml in methanol/water (1:1, v/v) were shown in Figure 60A and 60B. As shown in Figure 60A, the HPLC of TE showed the main peak around 60 min and few peaks of the minor compounds, while that of GSE showed not a few peaks in addition to the main peak. The large area of the main peak in TE than that in GE showed the higher content of the main peak in TE than that in GE. In Figure 60B, the HPLC chromatograms of the LH20 purified samples of both TE and GE from a commercial product were shown. Both samples showed nearly one peak.

The calibration curves of polymeric proanthocyanidins purified with LH20 were obtained with high linearity ($R^2 > 0.991$): $y = 2.40 \times 10^7 x - 2363707$ for GE: $y = 1.37 \times 10^7 x + 3694501$ for TE, where y = peak area and x = polymeric proanthocyanidins (mg/ml). These calibration curves were used for the determination of the content of polymeric proanthocyanidins of the samples.

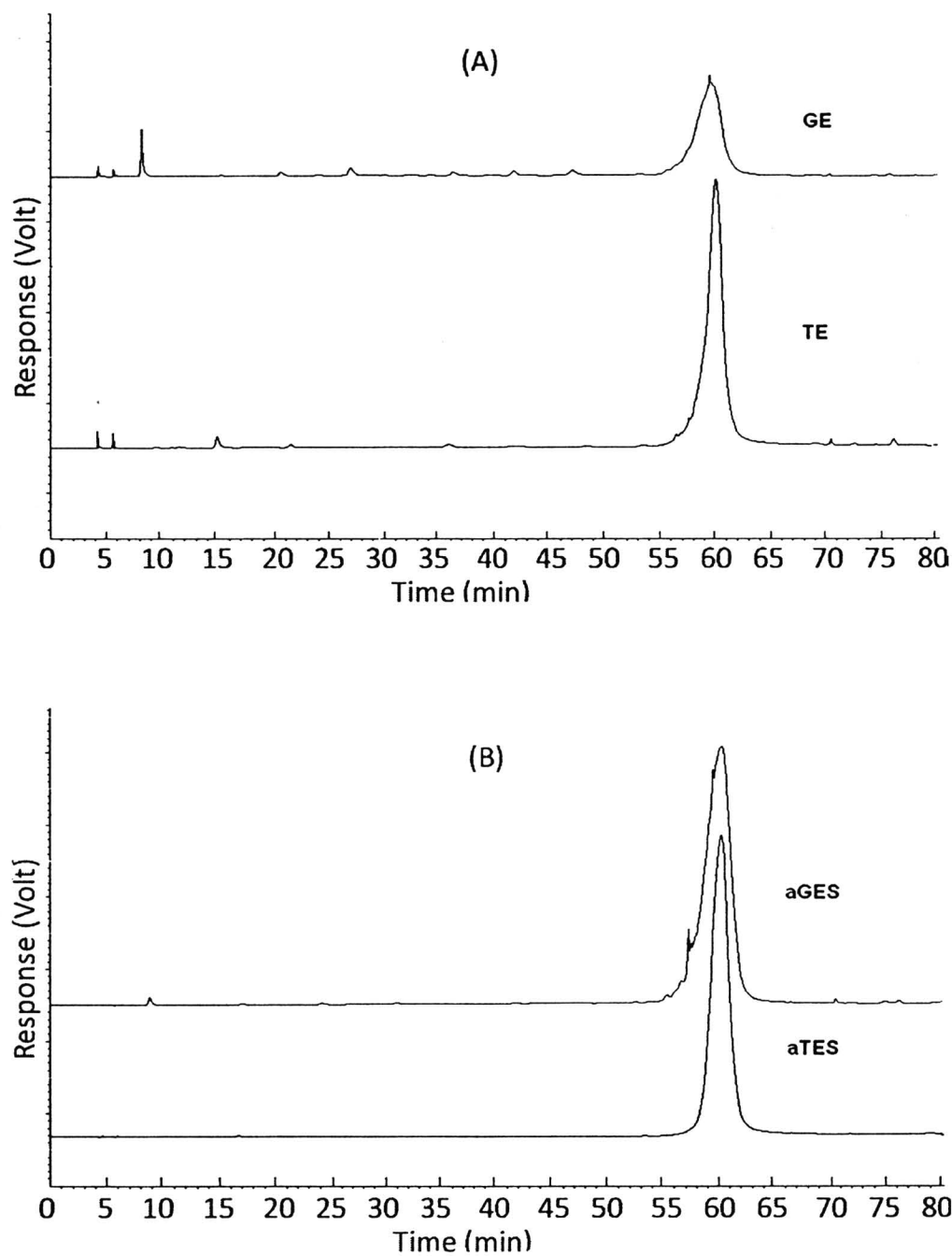


Figure 60 Reverse-phase HPLC chromatograms of (A) crude tamarind seed husk ethanolic extract (TE) and crude grape seed ethanolic extract (GE); (B) purified aTES and purified aGES using gradient of 0.03% trifluoroacetic acid and acetonitrile as mobile phase. Concentration of the samples was 5 mg/ml in methanol.

Structural characterization of polymeric proanthocyanidins in aTES

1. Structural characterization of polymeric proanthocyanidins in aTES by ^{13}C -NMR spectroscopy

^{13}C -NMR spectra of polymeric proanthocyanidins of aTES and aGES, purified with Sephadex LH 20 were shown in Figure 61. The assignment was made based on the publications of Czochanska, et al.(1980), Kennedy and Jones.(2000), and Kennedy, et al. (2001). ^{13}C -NMR spectra of polymeric proanthocyanidins of aTES and aGES were almost identical representing all the necessary signals for polymeric tannins consisting of flavan-3-ols (condensed tannins). Therefore, the chemical structure of polymeric tannins of TSH was confirmed to belong to the condensed tannins containing PC and PD units.

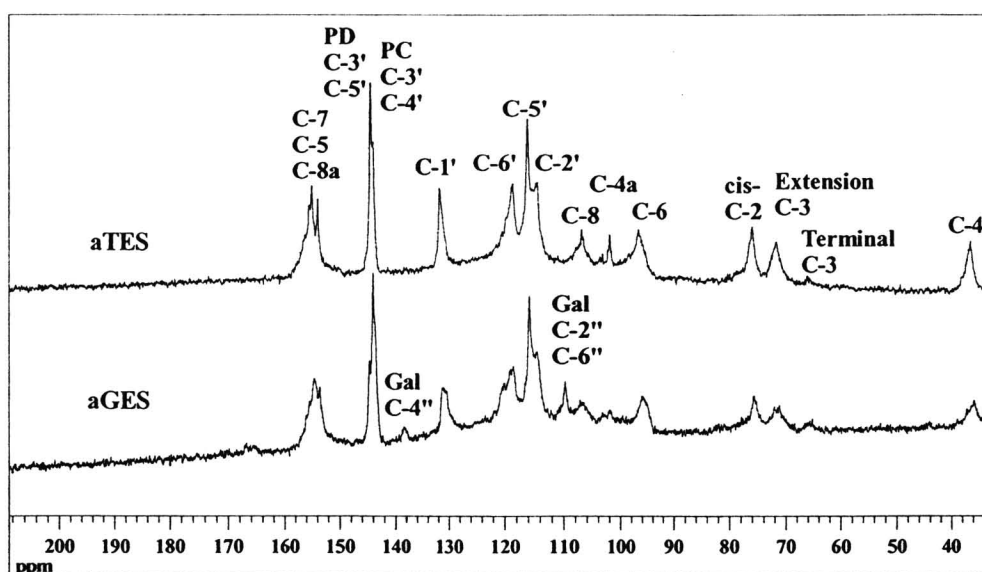


Figure 61 ^{13}C -NMR spectra for polymeric proanthocyanidins of aTES and aGES.

Table 13 ^{13}C -NMR chemical shifts of polymeric proanthocyanidins (PA) from aTES and aGES

Structure	Polymeric PA of aTES (ppm)	Polymeric PA of aGES (ppm)
Flavan-3-ol unit		
C-2	77.1	77.6
C-3(terminal unit)	67.0	66.5
C-3(extension unit)	71.8	71.2
C-4	36.5	35.9
C-4a	102.0	102.1
C-5	153.9-159.0	152.4-157.7
C-6	96.7	96.1
C-7	153.9-159.0	152.4-155.7
C-8	106.9	107.2
C-8a	153.9-159	152.4-157.7
C-1'	131.9	131.1
C-2'	114.5	114.7
C-3' of PC ^a	144.6	144.0
C-3' of PD ^b	145.6	144.6
C-4' of PC	144.6	144.0
C-4' of PD	131.9	131.1
C-5' of PC ^c	116.2	115.8
C-5' of PD ^d	145.6	144.6
C-6'	118.7	118.6
Galloyl unit		
C-1''	nd ^e	131.1
C-2''	nd	109.7
C-3''	nd	144.0
C-4''	nd	138.6
C-5''	nd	144.6
C-6''	nd	109.7

Remark: ^aPC = procyanidins, ^bPD = prodelphinidins, ^cnon-substituted aromatic carbon, ^dsubstituted aromatic carbon with OH, ^enot detected.

Through the purification of TE with sephadex LH20, the composition of TE was found to be $25.2 \pm 0.9\%$ (w/w) of mTES and $73.9 \pm 1.5\%$ (w/w) of aTES from the three different experiments. On the other hand, the content of polymeric proanthocyanidins in crude TSE was about 88-95% (Table 12). These results suggested that mTES should contain a high amount of polymeric proanthocyanidins. The HPLC chromatogram and the ^{13}C -NMR of mTES were shown in Figure 62. The content of polymeric proanthocyanidins in mTES was calculated from HPLC analysis using aTES as a standard and found to be about 79% (w/w). The ^{13}C -NMR of mTES was very similar to that of aTES, showing all the carbons necessary for polymeric proanthocyanidins. Therefore, the main ingredient of mTES was confirmed to be condensed tannin similar to aTES.

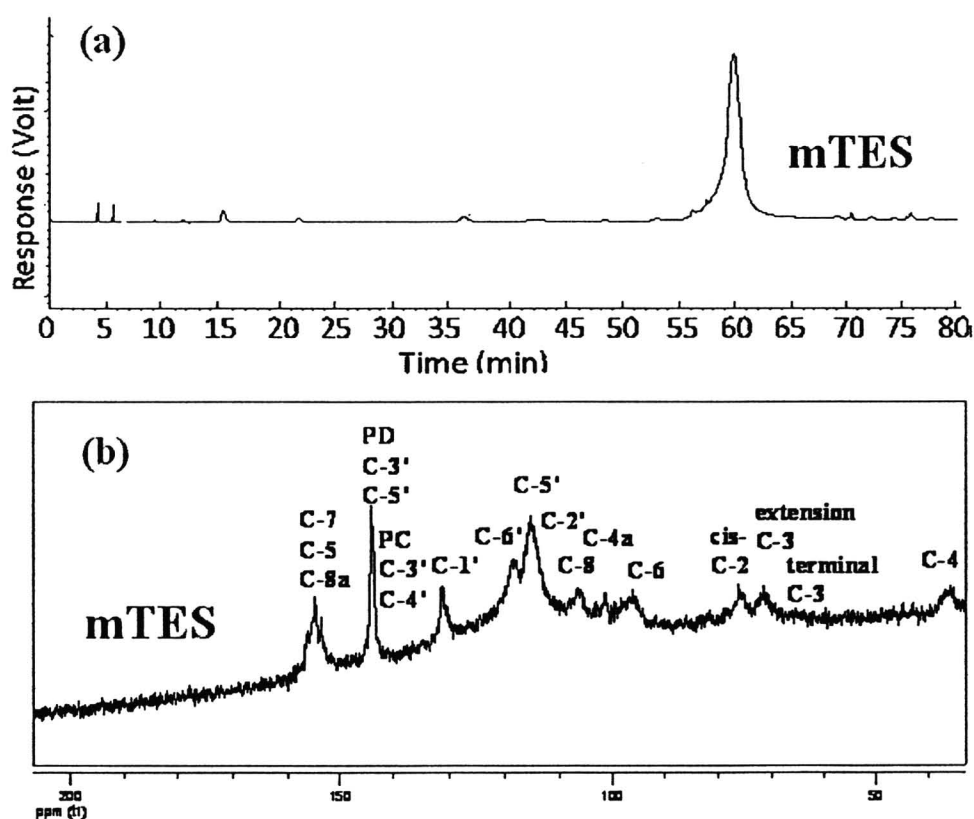


Figure 62 (a) Reverse-phase HPLC profiles and (b) ^{13}C -NMR spectra of mTES.

2. Degree of Polymerization (DP) of polymeric proanthocyanidins from aTES and aGES

The DP of polymeric proanthocyanidins of aTES and aGES, which were measured by vanillin assay, were 7.1 ± 0.3 and 6.2 ± 0.2 . The DP of GSE was in the range of the reported values of DP of GS, which were 8.1 for Cabernet franc (Labarbe *et al.*, 1999), 5.6 and 8.3 for Cabernet Sauvignon (Kennedy, *et al.*, 2000), 3.4-3.6 for Merlot (Saucier, *et al.*, 2001), 4.4 for Shiraz, 2.6 for Chardonnay (Kennedy & Jones, 2001).

3. UV and IR spectrometry of polymeric proanthocyanidins from aTSE and aGSE

The UV spectra of aTES and aGES at $40 \mu\text{g/ml}$ in methanol were shown in Figure 63. Both polymeric proanthocyanidins of aTES and aGES showed the same maximum absorption at 280nm. Polymeric proanthocyanidins of aGES showed the larger intensity in absorbance than that of aTES (Figure 64), which was attributed to the difference in PD/PC of aTES and aGES.

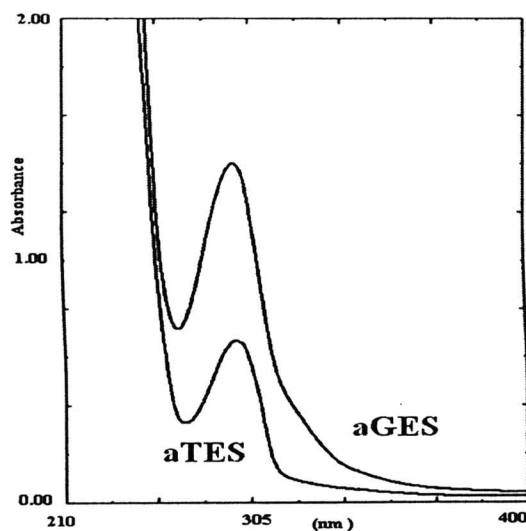


Figure 63 UV spectra of aTES and aGES at $40 \mu\text{g/ml}$ in methanol.

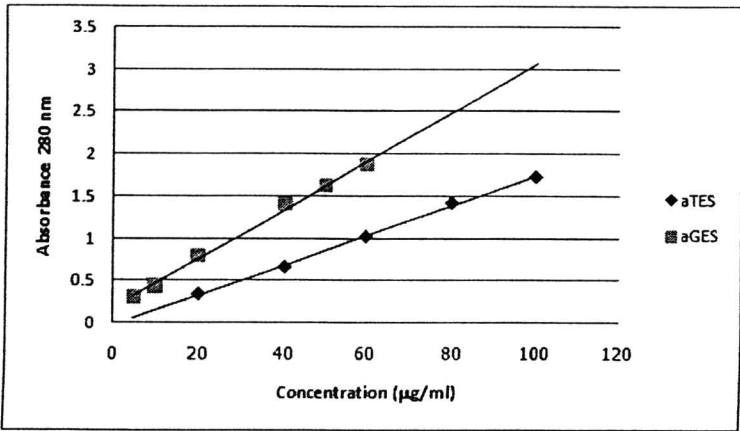


Figure 64 UV absorption curves of aTES and aGES in various concentration at 280 nm

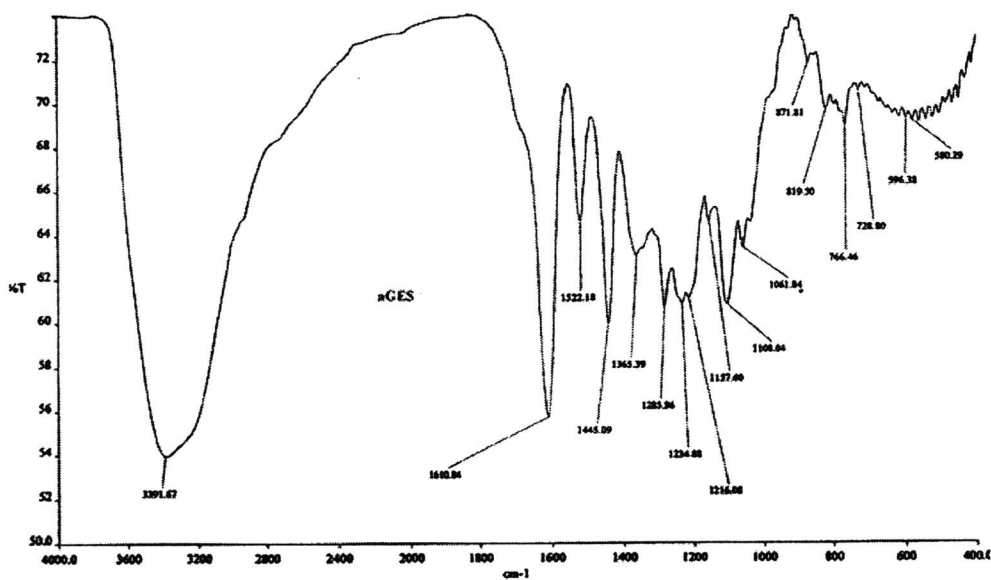


Figure 65 Infrared spectrums of polymeric proanthocyanidins in aGES using KBr disc

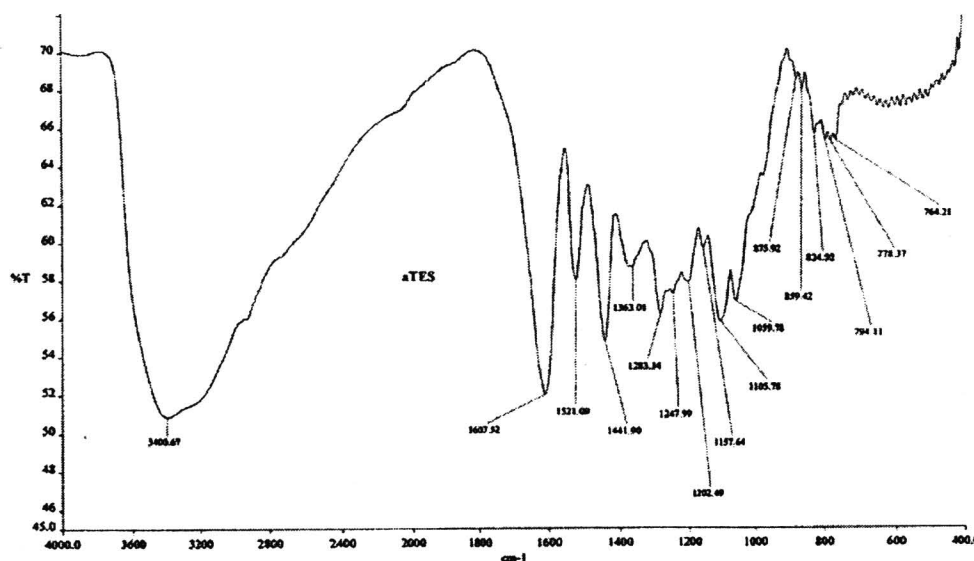


Figure 66 Infrared spectrums of polymeric proanthocyanidins in aTES using KBr disc

The IR spectra of polymeric proanthocyanidins of aTES (Figure 66) and aGES (Figure 65) were similar though the IR of polymeric proanthocyanidins of aGES showed the shoulder peak around 1700 cm^{-1} , suggesting the C=O stretch of galloyl ester (data not shown).

4. Antioxidant activities of polymeric proanthocyanidins from aTES and aGES

The IC_{50} values of polymeric proanthocyanidins of aTES and aGES were $4.2 \pm 0.2\text{ }\mu\text{g/ml}$ and $3.2 \pm 0.2\text{ }\mu\text{g/ml}$ (DPPH assay), $6.2 \pm 0.3\text{ }\mu\text{g/ml}$ and $6.0 \pm 0.1\text{ }\mu\text{g/ml}$ (ABTS assay), respectively. The antioxidant and the radical scavenging activities of polymeric proanthocyanidins of aTES and aGES were similar, showing that the differences in the chemical structures between polymeric proanthocyanidins of aTES and aGES had not an effect on the antioxidant activities.